CORE
Metadata, citation and similar papers at core.ac.uk
Provided by Woods Hole Open Access Server

Geochemistry Geophysics Geosystems G3

Article
Volume 12, Number 10
4 October 2011
Q0AB11, doi:10.1029/2011GC003699
ISSN: 1525-2027

Published by AGU and the Geochemical Society

Insight into volatile behavior at Nyamuragira volcano (D.R. Congo, Africa) through olivine-hosted melt inclusions

Elisabet M. Head
Department of Geological and Mining Engineering and Sciences, Michigan Technological University, Houghton, Michigan 49931, USA (emhead@mtu.edu)

Alison M. Shaw
Geology and Geophysics Department, Woods Hole Oceanographic Institution, Woods Hole, Massachusetts 02543, USA (ashaw@whoi.edu)

Paul J. Wallace
Department of Geological Sciences, University of Oregon, Eugene, Oregon 97403, USA (pwallace@uoregon.edu)

Kenneth W. W. Sims
Department of Geology and Geophysics, University of Wyoming, Laramie, Wyoming 82071-2000, USA (ksims7@uwyo.edu)

Simon A. Carn
Department of Geological and Mining Engineering and Sciences, Michigan Technological University, Houghton, Michigan 49931, USA (scarn@mtu.edu)

[1] We present new olivine-hosted melt inclusion volatile (H_2O, CO_2, S, Cl, F) and major element data from five historic eruptions of Nyamuragira volcano (1912, 1938, 1948, 1986, 2006). Host-olivine Mg#'s range from 71 to 84, with the exception of the 1912 sample (Mg# = 90). Inclusion compositions extend from alkali basalts to basanite-tephrites. Our results indicate inclusion entrapment over depths ranging from 3 to 5 km, which agree with independent estimates of magma storage depths (3–7 km) based on geophysical methods. Melt compositions derived from the 1986 and 2006 Nyamuragira tephra samples best represent pre-eruptive volatile compositions because these samples contain naturally glassy inclusions that underwent less post-entrapment modification than crystallized inclusions. Volatile concentrations of the 1986 and 2006 samples are as follows: H_2O ranged from 0.6 to 1.4 wt %, CO_2 from 350 to 1900 ppm, S from 1300 to 2400 ppm, Cl from 720 to 990 ppm, and F from 1500 to 2200 ppm. Based on FeO_T and S data, we suggest that Nyamuragira magmas have higher fO_2 (>NNO) than MORB. We estimate the total amount of sulfur dioxide (SO_2) released from the 1986 (0.04 Mt) and 2006 (0.06 Mt) Nyamuragira eruptions using the petrologic method, whereby S contents in melt inclusions are scaled to erupted lava volumes. These amounts are significantly less than satellite-based SO_2 emissions for the same eruptions (1986 = ~1 Mt; 2006 = ~2 Mt). Potential explanations for this observation are: (1) accumulation of a vapor phase within the magmatic system that is only released during eruptions, and/or (2) syn-eruptive gas release from unerupted magma.

Components: 13,400 words, 8 figures, 3 tables.

Keywords: effusive volcanism; eruption mechanisms; excess sulfur; melt inclusions; volcanic gases.

Index Terms: 8415 Volcanology: Intra-plate processes (1033, 3615); 8425 Volcanology: Effusive volcanism (4302); 8430 Volcanology: Volcanic gases.

Copyright 2011 by the American Geophysical Union

Received 12 May 2011; **Revised** 9 August 2011; **Accepted** 10 August 2011; **Published** 4 October 2011.

Head, E. M., A. M. Shaw, P. J. Wallace, K. W. W. Sims, and S. A. Carn (2011), Insight into volatile behavior at Nyamuragira volcano (D.R. Congo, Africa) through olivine-hosted melt inclusions, *Geochem. Geophys. Geosyst.*, *12*, Q0AB11, doi:10.1029/2011GC003699.

Theme: Magma-Rich Extensional Regimes
Guest Editors: R. Meyer, J. van Wijk, A. Breivik, and C. Tegner

1. Introduction

[2] Volatiles in magma play a key role in the timing, magnitude, and style of volcanic eruptions [e.g., *Parfitt and Wilson*, 1994; *Sparks*, 1997; *Sutton et al.*, 2001; *Edmonds and Gerlach*, 2007; *Shinohara*, 2008], and can provide valuable insight into the depth and source of magma, whether the conduit is open or sealed and, potentially, the rate at which magma is erupting [e.g., *Greenland et al.*, 1985; *Sutton et al.*, 2001]. Studies of volcanic degassing typically focus on either volatiles within the pre-eruptive magma or on gas emissions between or during eruptions. Here, we evaluate the dynamics of volcanic degassing through a combination of volcanic gas emissions, melt inclusion compositions, and associated erupted lava volumes. Melt inclusions are tiny droplets of magma trapped in growing crystals that are brought to the surface during eruption in lava flows or tephra deposits. The crystal serves as a pressure vessel, essentially preserving the original composition of the trapped magma, assuming that diffusion has not modified the composition significantly [see *Gaetani and Watson*, 2000; *Spandler et al.*, 2007; *Portnyagin et al.*, 2008]. Olivine-hosted inclusions are often targeted since olivine is an early crystallizing phase, thus magma compositions over a range of depths (pressures) can be recorded. This allows pre-eruptive magma to be "sampled" from deep to shallow depths in the system. Pre-eruptive magma volatile concentrations derived from melt inclusion studies provide insight into crystallization processes, magma storage depths, and how volatiles contribute to magma ascent and eruption [*Anderson*, 1974; *Devine et al.*, 1984; *Dunbar et al.*, 1989; *Wallace et al.*, 1999; *Wallace*, 2001; *Roggensack*, 2001; *Metrich et al.*, 2004].

[3] Volcanic gas emissions, on the other hand, are typically measured via ground- or satellite-based remote sensing methods. Satellite-based techniques are particularly useful for remote or hazardous volcanoes and large eruptions, but are usually restricted to measurements of sulfur dioxide (SO_2), because the other dominant volcanic gases (water (H_2O) and carbon dioxide (CO_2)) are difficult to resolve from the atmospheric background. Here we examine the relationship between satellite-based volcanic SO_2 emissions measurements and SO_2 emissions derived from sulfur concentrations in melt inclusions coupled with magma eruption volumes.

[4] Previous studies of basaltic eruptions in hot spot-related localities such as Hawaii and Iceland have suggested that remote sensing SO_2 flux estimates are similar to those derived from melt inclusion S concentrations combined with erupted magma volumes (petrologic method [e.g., *Gerlach et al.*, 1996; *Wallace*, 2001; *Sharma et al.*, 2004]). However, for more silicic volcanic eruptions such as the 1991 Pinatubo eruption (Philippines), and for some mafic arc volcanoes, the SO_2 emissions measured via satellite remote sensing often greatly exceed sulfur yields predicted from petrological data [*Wallace and Gerlach*, 1994; *Wallace*, 2001; *Witter et al.*, 2005]. This inequality, known as "excess sulfur," has been attributed to the presence of an exsolved vapor phase in the magma prior to eruption [*Wallace*, 2001; *Shinohara*, 2008]. Although explosive eruptions of silicic arc magmas are more typically associated with excess sulfur, preliminary studies of SO_2 emissions and lava production for effusive basaltic hot spot and rift eruptions suggest that excess sulfur emissions may also occur in non-arc settings. In this contribution, we test the hypothesis using data from Nyamuragira volcano (1.408°S, 29.20°E; 3058 m), located in the extensional tectonic setting of the East African Rift. We focus on Nyamuragira's SO_2 emissions, comparing satellite-based remote sensing fluxes with those derived using the petrologic technique, and show that its SO_2 emissions are significant and cannot be reconciled with the amount of erupted lava.

[5] Nyamuragira volcano, located in the Virunga region of the Democratic Republic of the Congo (D.R. Congo; Figure 1), is one of the most active volcanoes in Africa, with 16 effusive eruptions

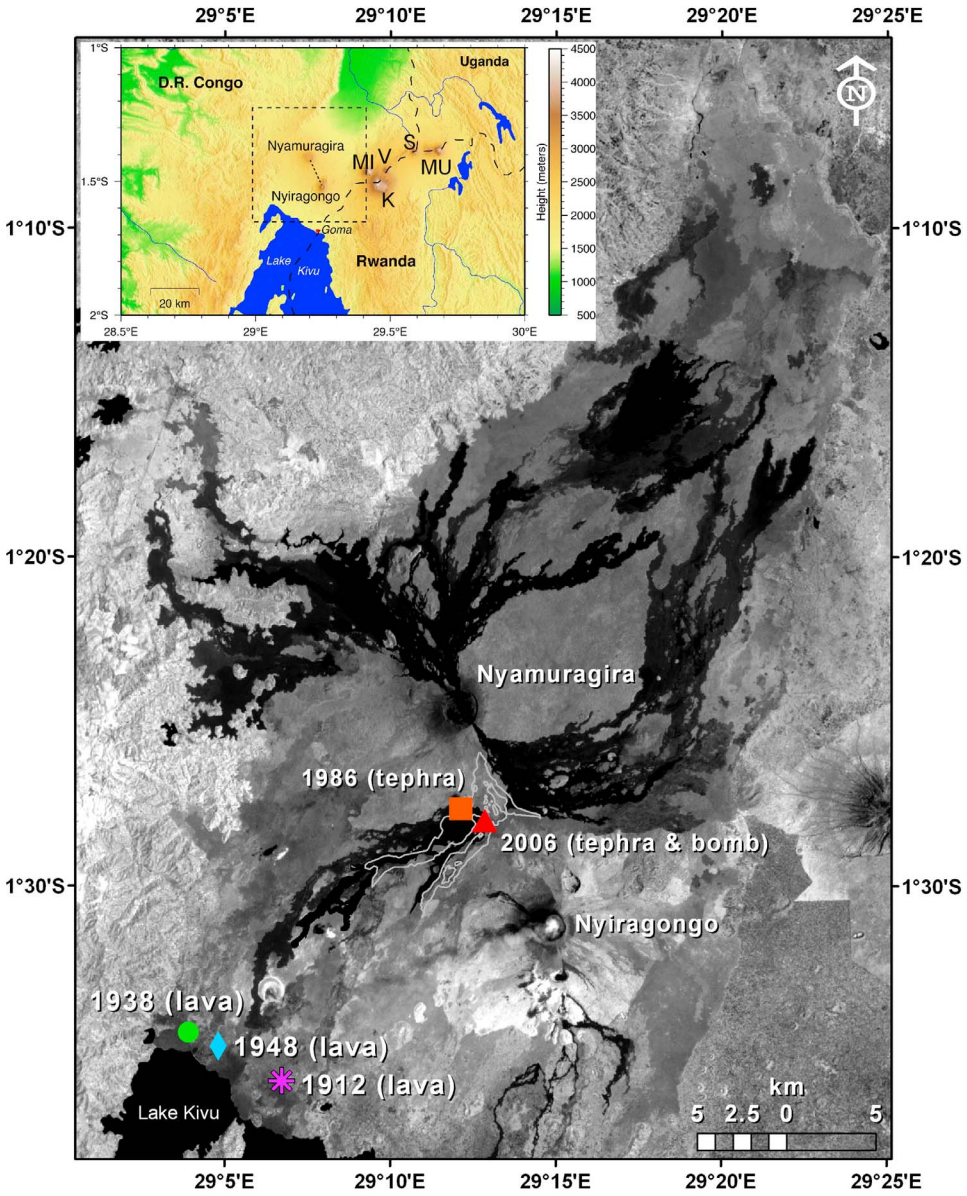

Figure 1. Location of Nyamuragira (D.R. Congo) within the western branch of the East African Rift near the Rwandan border. Sample locations are marked by eruption year and symbols correspond to the data presented in all figures. The base map is a Landsat image acquired on 21 February 2005 with the 2006 and an outline of the 2010 lava flows superimposed (from E. M. Head et al., manuscript in preparation, 2011). The inset SRTM image shows the locations of volcanoes within the Virunga chain: Mu- Muhavura, S- Sabinyo, V- Visoke, Mi- Mikeno, and K- Karisimbi, as well as the NNW-SSE rift zone (dotted line), which has been linked to regional tectonic stresses. Nyamuragira eruptions since 1996 have occurred along this zone.

between 1980 and 2010. Due to the difficulties of ground-based work owing to the region's adverse political climate, volcanic gas emissions from Nyamuragira have been evaluated via satellite methods [*Carn and Bluth*, 2003; *Bluth and Carn*, 2008]. Satellite-based measurements of global volcanic SO_2 began in 1978 with the launch of the ultraviolet (UV) Total Ozone Mapping Spectrometer (TOMS [*Krueger*, 1983]). The Ozone Monitoring Instrument (OMI) continued UV space-based monitoring of volcanic SO_2 emissions from September 2004, overlapping TOMS measurements for ~16 months, until the end of the TOMS mission in 2005 [*Krotkov et al.*, 2006; *Yang et al.*, 2007]. Based on TOMS data, SO_2 emissions from Nyamuragira's frequent effusive eruptions were found to comprise

a significant fraction (~10%) of the global volcanic sulfur budget [*Halmer et al.*, 2002]; it is estimated that ~25 Mt of SO_2 was released from Nyamuragira into the atmosphere between 1980 and 2004 [*Bluth and Carn*, 2008].

[6] Nyamuragira erupts low-silica, alkalic lavas, including alkali basalts, hawaiites, basanites and tephrites (SiO_2 = 43–56 wt%, K_2O + Na_2O up to 7 wt% [*Aoki et al.*, 1985]). It erupts very fluid lava that can achieve flow rates of up to ~20 km/h [*Smithsonian Institution*, 1982]. *Bluth and Carn* [2008] suggested that syn-eruptive SO_2 emissions from Nyamuragira may correlate with effusive lava emissions. Hence, understanding the link between SO_2 emissions and erupted lava is important for future monitoring and hazard assessment and to further our understanding of degassing and eruption mechanisms at Nyamuragira. In addition, evolved alkalic melts have been important carriers of sulfur to the atmosphere in several globally significant eruptions, such as Tambora in 1815 (phonolite), Vesuvius in 79 AD (phonolite), Laacher See in 12900 BP (phonolite), and El Chichon in 1982 (trachyandesite) [*Self et al.*, 1984; *Schmincke et al.*, 1999; *Harms and Schmincke*, 2000]. Investigation of sulfur behavior in less evolved alkaline magmas such as those erupting at Nyamuragira could illuminate the origin of volatiles released by these eruptions, several of which have been linked to global climate variations. Furthermore, ascertaining the connection between melt inclusion S concentrations and S emissions in alkaline magmas is important when evaluating whether melt inclusions are accurately describing the S release, as they do for many tholeiitic basaltic eruptions.

[7] Previous studies of Nyamuragira volcanic products have focused on the physical, major and trace element, and isotope characteristics of lavas and tephras [*Denaeyer*, 1969; *Pouclet*, 1975; *Kampunzu et al.*, 1984; *Aoki et al.*, 1985; *Hayashi et al.*, 1992; *Chakrabarti et al.*, 2009a]. Volatile studies of Nyamuragira magmas, on the other hand, are currently lacking. Here we present new volatile (H_2O, CO_2, S, Cl, F) and major element data from olivine-hosted melt inclusions from six Nyamuragira lava and tephra samples from five historic eruptions (1912, 1938, 1939, 1986, and 2006). These results are then compared to SO_2 emissions derived from TOMS and OMI data. Given the significance of Nyamuragira to present-day global volcanic gas emissions, it is important to understand the role of volatiles in Nyamuragira's eruptions. Our work constitutes the first reported analysis of melt inclusions in magmas from an active segment of the East African Rift (EARS) system; the only other similar study known to us reported preliminary data from Turkana [*Waters et al.*, 2004].

2. Geologic Setting and Eruption Characteristics

[8] The first volcanic activity associated with the East African Rift occurred 45 Ma in Ethiopia and propagated south to Kenya, where the rift split around the Tanzanian craton into eastern and western branches [*George et al.*, 1998]. Volcanism in the western branch began 11 Ma and its eruptive products are less voluminous, more potassic, and silica-undersaturated compared to those from the eastern branch [*Kampunzu et al.*, 1998; *Furman and Graham*, 1999; *Furman*, 2007]. The western branch spans ~750 miles between Lakes Albert and Malawi and can be broken up into four volcanic regions from north to south: (1) Toro-Ankole in western Uganda, (2) Virunga and (3) Kivu spanning the D.R. Congo, Rwanda, Burundi, and southern Uganda, and (4) the Rungwe in southern Tanzania [*Ebinger*, 1989; *Furman*, 1995; *Rogers et al.*, 1998; *Kampunzu et al.*, 1998; *Furman and Graham*, 1999; *Spath et al.*, 2001; *Ebinger and Furman*, 2002; *George and Roger*s, 2002; *Furman et al.*, 2004].

[9] Nyamuragira and its neighboring volcano, Nyiragongo, are currently the only active volcanoes in the western branch and are part of the Virunga volcanic chain. The less active volcanoes within this chain are, from northeast to southwest, Muhavura, Sabinyo, Visoke, Karisimbi, and Mikeno (Figure 1), with the last eruptive activity from Visoke in 1957. Nyamuragira, Muhavura, Karisimbi, and Mikeno have erupted similar lava compositions consisting of K-basanites with evolved derivatives [*Rogers et al.*, 1998]. In contrast, Sabinyo has erupted silica-rich lavas (K-trachytes and latites), which are suggested to have evolved from K-basanites through crustal mixing [*Rogers et al.*, 1998]. Nyiragongo produces more extreme compositions of leucite-bearing nephelinites and melilitites [*Platz et al.*, 2004]. Using both Nd-Sr-Pb and ^{238}U-^{230}Th-^{226}Ra-^{120}Pb isotopic data from Nyiragongo lavas, *Chakrabarti et al.* [2009a, 2009b] suggested that Nyiragongo magmas are generated at greater mantle depths and lower degrees of partial melting than Nyamuragira. The last flank eruption from Nyiragongo occurred in 2002, and a lava lake now occupies its summit crater [*Tedesco et al.*, 2007].

[10] Volcanism at Nyamuragira since 1948 has been dominated by episodic flank effusive eruptions with intervals of summit lava lake activity

Table 1 (Sample). Whole Rock Major and Select Trace Elements[a] [The full Table 1 is available in the HTML version of this article]

Sample	SiO_2	TiO_2	Al_2O_3	FeO_T	MnO	MgO	CaO	Na_2O	K_2O	P_2O_5	Ni	Cr	Sc†	V	Ba†	Rb†	Sr†
1948 (lava)	45.75	3.72	16.32	12.00	0.20	4.93	9.48	3.41	3.56	0.64	33	31	16	311	1080	93	1071
1938 (lava)	45.92	3.76	16.38	11.73	0.20	4.66	9.67	3.41	3.60	0.65	27	25	16	311	1104	95	1100
1912 (lava)	45.26	2.71	10.21	10.55	0.17	13.52	13.73	1.81	1.72	0.33	275	724	44	316	527	44	598
2006 (bomb)	45.82	3.55	15.52	11.76	0.20	5.56	11.29	2.92	2.82	0.54	26	21	25	356	900	76	933
2006 (tephra)	45.94	3.55	15.54	11.63	0.20	5.55	11.30	2.93	2.82	0.54	25	20	26	353	900	76	938
1986 (tephra)	46.30	3.70	16.08	11.82	0.20	4.99	10.26	2.81	3.24	0.61	22	19	21	341	1034	87	1026

[a]All samples were analyzed by XRF methods for major and trace elements, and ICP-MS (†) methods for a larger suite of trace elements.

[*Hamaguchi and Zana*, 1983]. Twenty-six eruptions have occurred over the last 62 years with an average inter-eruptive repose period of ~3 years since 1980 [*Burt et al.*, 1994]. Activity typically begins with fire fountains ~200 m in height from one or more fissure vents, and most of the lava volume is issued in the early stage of the eruption. Hawaiian-type fire fountaining often changes to Strombolian-type activity later in the eruption [*Ueki*, 1983] (Smithsonian Institution, monthly reports for Nyamuragira, 1971–2010, http://www.volcano.si.edu/world/volcano.cfm?vnum=0203-02=&volpage=var, hereinafter referred to as Smithsonian Institution, monthly reports, 1971–2010 [e.g., *Smithsonian Institution*, 1982, 2006]). Vents for Nyamuragira flank eruptions tend to cluster along a major line of weakness, which extends from the summit caldera (Figure 1). Since 1996, most eruptions have originated from this NW-SE rift zone that has been shown to align with the axis of maximum extensional strain in the region [*Pouclet and Villeneuve*, 1972; *Kasahara*, 1983; *Zana*, 1983; *Chorowicz et al.*, 1987]. Geophysical data (seismicity and tilt) have been used to infer the existence of a magma chamber at a depth of ~3–7 km beneath Nyamuragira [*Hamaguchi*, 1983]. An aseismic zone was found between clusters of short-period earthquakes at 0–3 km depths and long-period earthquakes at 7–16 km depths. Modeling of benchmark and tiltmeter data corroborate the location and depth of this aseismic zone, which is considered to be Nyamuragira's magma reservoir [*Hamaguchi*, 1983; *Kasahara*, 1983].

3. Analytical Techniques

[11] Major and trace element whole rock compositions of Nyamuragira lava samples (1912, 1938, and 1948 eruptions), tephra samples (1986 and 2006 eruptions), and a 2006 bomb sample were determined by X-Ray Fluorescence (XRF) and Inductively Coupled Plasma-Mass Spectrometry (ICP-MS) at the GeoAnalytical Laboratory at Washington State University (Table 1).

[12] Lava and tephra samples (Figure 1) were crushed, sieved, and handpicked for olivine crystals. The olivines were placed in ethanol and then examined under a binocular microscope to identify suitable melt inclusions. All olivine-hosted melt inclusions from the lava samples were devitrified, with the exception of one naturally glassy inclusion in the 1912 sample. The 1986 and 2006 tephra samples contained naturally glassy melt inclusions, but nothing suitable was found in the 2006 bomb sample. A total of 34 inclusions ranging in size from ~15 to 150 μm were selected for study, and 11 out of the 34 contained spherical vapor bubbles with diameters between 6 and 33 μm. An effort was made to select only melt inclusions that were fully enclosed within the olivine to minimize selection of inclusions affected by late-stage volatile loss.

[13] Although the lava flow samples contained abundant olivine and pyroxene crystals, most melt inclusions were devitrified (crystalline) and, therefore, these inclusions were rehomogenized following the approach described by *Roedder* [1979, 1984] and *Danyushevsky et al.* [2002]. We recognize that both the crystallization process and the re-homogenization processes have the potential to modify volatile composition. Rehomogenization can result in H_2O loss due to H diffusion upon reheating [e.g., *Massare et al.*, 2002]. However, we used temperatures ≤1200°C and the samples were reheated for ≤15 min. These time constraints during reheating experiments have been shown to minimize H_2O-loss considerably [*Sobolev et al.*, 1983; *Danyushevsky et al.*, 2002; *Rowe et al.*, 2007] (see discussion in section 4.2). To estimate crystallization temperatures (maximum temperature of heating) for the re-homogenization experiments, we used the major element composition of representative olivines from each lava flow sample and the geothermometer of *Roeder and Emslie* [1970]. Olivines from each sample were heated to the

estimated crystallization temperature (1150–1200°C) in a Deltech furnace with oxygen fugacity maintained at FMQ (fayalite-magnetite-quartz buffer) for no longer than 15 min following *Rowe et al.* [2007]. The olivines were then released into a beaker of water to quench the inclusions. Only melt inclusions from the 1912 sample did not appear to revitrify after heating and quenching, perhaps because of an inaccurate crystallization temperature estimate.

[14] Naturally glassy melt inclusions from the 1986 and 2006 tephra samples, as well as reheated 1938 and 1948 inclusions with ≤50 μm diameters, were prepared for SIMS analyses. Olivines were mounted in epoxy and hand polished to expose the inclusions on one side. The olivines were then removed from epoxy mounts, cleaned, mounted in indium metal, and polished for ion and electron microprobe analyses. The indium-mounted inclusions were then analyzed with the 1280 ion microprobe (H_2O, CO_2, S, Cl, and F) at Woods Hole Oceanographic Institution following methods described by *Shaw et al.* [2010]. A 15–20 μm rastered spot was measured with a 1–2 nA Cs^+ beam. Combined accuracy and precision is ~10% (2σ) and detection limits for H_2O, CO_2, S, Cl, and F are 100, 8, 8, 2, and 1 ppm, respectively.

[15] A subset of 1938 and 1948 reheated melt inclusions, as well as the 1912 glassy inclusion, were also analyzed for H_2O and CO_2 using infrared (IR) spectroscopy at the University of Oregon. Only inclusions ≥50 μm in diameter were analyzed because analytical uncertainties are much larger for smaller inclusions. Descriptions of sample preparation and analytical methods are given by *Vigouroux et al.* [2008] and *Johnson et al.* [2008]. We used *Dixon and Pan* [1995] to determine the compositionally dependent molar absorption coefficients for the carbonate peaks, and we used an absorption coefficient of 63 L/mol cm for the fundamental O-H stretching vibration [*Dixon et al.*, 1995].

[16] Major and volatile (S, Cl, and F) element compositions of the melt inclusions, tephra glasses, and olivine host crystals were determined using the Cameca SX-100 electron microprobe at the University of Oregon and the JEOL-JXA-733 electron microprobe at the Massachusetts Institute of Technology (MIT) (Table 2). At the University of Oregon, a 15 kV accelerating voltage and a spot size of 20 μm was used. Beam current was 10 nA for Na, Si, K, Al, Mg, Fe, and Ca, and 50 nA for F, S, Cl, Ti, Mn, and P. The counting time was 20 s for Mn, 40 s for K, Ca, F, and Si, 60 s for Mg, Al, and P, 80 s for Na and Ti, 96 s for S, 100 s for Cl, and 120 s for Fe. At MIT, a 15 kV accelerating voltage, 10 nA beam intensity, and a spot size of 1–10 μm was used. Counting times were 5 s for Na and 40 s for all other elements. Each olivine grain was measured 3 times at variable distances from the melt inclusion to evaluate the presence of compositional zoning. We found uniform olivine compositions at all distances from the inclusion, suggesting that our olivines are not zoned.

[17] All melt inclusion data were corrected for post-entrapment crystallization (PEC) of olivine along the walls of the inclusion. Equilibrium olivine was added in 0.1 wt% increments to melt inclusion compositions until they were in equilibrium with their host olivine. An Fe-Mg K_d [$(FeO/MgO)_{olivine}/(FeO/MgO)_{melt\ inclusion}$] of 0.3 was used, and we assumed that 30% of the total Fe was present as Fe^{3+}. On average, 8% or less olivine was added back to the 1986 and 2006 tephra samples. For the rehomogenized samples, however, a range of −11% to 11% olivine was added (Table 3). Negative values indicate that the olivine was heated to a higher temperature than its trapping temperature during the rehomogenization process or, alternatively, large amounts of cooling between inclusion entrapment and eruption, especially for melt inclusions in high-Fo olivine, could have occurred [*Danyushevsky et al.*, 2000; *Johnson et al.*, 2010]. We also corrected 9 inclusions for shrinkage bubble formation to determine the amount of gas present in the bubble [see *Shaw et al.*, 2008]. Through this process, H_2O and CO_2 are added back to the mass of the inclusion. In all cases, this correction resulted in a <0.01 wt% change in water concentrations. Carbon dioxide corrections, on the other hand, resulted in an 11–46% change between the original and corrected values.

4. Results

4.1. Major and Minor Element Chemistry

[18] The Virunga volcanoes have produced lava compositions ranging from melilitites to basanites to trachyandesites. Based on major element melt inclusion and whole rock compositions (Tables 1 and 3), our Nyamuragira samples fall within the basanite-tephrite and alkali basalt fields on the total alkali versus silica diagram, and are within the range of whole rock compositions previously determined [e.g., *Aoki and Yoshida*, 1983; *Aoki et al.*, 1985; *Hayashi et al.*, 1992]. The major element chemistry of melt inclusions can be used for evaluating

Table 2. Uncorrected Melt Inclusion Major Elements and Volatiles

Sample	SiO_2	TiO_2	Al_2O_3	FeO_T	MnO	MgO	CaO	Na_2O	K_2O	P_2O_5	H_2O (wt%)	CO_2 (ppm)	S (ppm)	Cl (ppm)	F (ppm)
2006 Eruption															
NYA0705-1	44.09	3.41	15.17	11.66	0.19	5.16	11.38	3.21	2.09	0.55	1.34	878	2254	822	1530
NYA0705-4a	45.37	3.61	16.12	11.21	0.19	3.43	11.55	3.04	2.25	0.44	1.25	950	2253	791	1527
NYA0705-4b	44.92	3.51	15.31	11.87	0.17	4.73	11.28	2.69	2.10	0.44	1.26	688	2154	768	1478
NYA0705-5b	43.84	3.42	15.05	11.31	0.22	3.53	12.80	2.42	1.97	1.27	1.24	650	2217	788	1554
NYA0705-9	45.06	3.43	15.41	12.00	0.19	4.50	11.18	2.93	2.19	0.45	1.28	852	2250	816	1542
NYA0705-10a	44.81	3.66	15.24	11.49	0.20	4.53	11.44	3.01	2.13	0.55	1.28	923	2145	802	1548
NYA0705-10b	44.73	3.35	15.37	11.92	0.17	4.35	11.56	3.09	2.16	0.48	1.16	827	2207	810	1550
NYA0705-12a	44.63	3.54	15.52	11.84	0.22	4.53	10.45	3.36	2.33	0.55	1.25	462	2325	842	1578
NYA0705-12b	44.69	3.68	15.60	11.87	0.16	4.23	11.69	3.04	2.19	0.47	1.29	1846	2183	787	1554
NYA0705-11	45.80	3.52	16.04	11.41	0.21	4.50	10.18	2.13	2.53	0.49	1.25	1460	2112	772	1500
1986 Eruption															
NYA0706-3a	47.16	3.25	16.68	10.95	0.22	3.94	8.81	1.96	3.53	0.55	1.33	1726	1953	953	2129
NYA0706-3b	46.31	3.62	16.18	10.20	0.21	4.23	11.70	3.13	1.88	0.47	0.89	409	1518	982	2147
NYA0706-4	45.70	3.42	15.90	11.59	0.24	4.17	9.96	2.92	2.65	0.56	1.05	1730	1271	848	1800
NYA0706-5	46.61	3.54	16.88	11.48	0.23	4.07	9.25	2.59	2.80	0.52	1.05	347	1868	821	1823
NYA0706-6	45.66	3.44	16.40	10.36	0.21	4.20	12.85	2.57	1.99	0.33	0.62	374	1813	870	1506
NYA0706-7	45.28	3.48	15.75	11.48	0.23	4.38	9.78	3.22	2.78	0.48	0.98	1690	1514	742	1755
NYA0706-10	46.17	4.27	16.74	10.38	0.26	3.22	10.83	2.58	2.73	0.37	1.43	1163	2057	922	1922
NYA0706-8	46.14	4.21	16.31	11.71	0.24	3.82	10.97	2.04	2.48	0.39	0.03	1448	1971	722	1849
1948 Eruption															
NYA-07-1	45.20	3.81	14.90	13.48	0.21	5.52	8.26	3.75	2.71	0.53	0.23	726	951	759	1896
NYA0701-3	43.80	3.30	14.86	14.81	0.26	5.34	9.32	4.46	2.63	0.46	0.23	880	1087	740	1678
NYA0701-7	43.80	3.41	14.51	15.54	0.25	5.52	8.21	3.59	2.61	0.49	0.13	31	331	82	2
NYA0701-15	44.56	2.60	17.52	11.09	0.22	6.24	8.85	3.42	2.41	0.39	0.17	848	1045	716	1818
NYA0701-4	44.75	2.77	17.42	11.28	0.25	5.90	9.25	3.39	2.40	0.33	0.14	238	694	563	1394
FTIR-Db	44.74	3.71	15.24	11.16	0.20	5.94	10.99	3.34	2.46	0.49	0.08	78	312	196	90
FTIR-G	44.42	3.65	15.93	11.28	0.18	6.17	9.86	3.29	2.61	0.47	0.15	4507	1303	796	1524
FTIR-B	43.51	3.55	15.78	12.11	0.24	5.74	10.20	3.70	2.55	0.48	0.13	651	1215	742	1572
FTIR-E	43.32	3.61	15.43	9.00	0.15	6.51	13.00	3.20	2.27	0.44	0.15	648	1379	751	1581
FTIR-Ca	44.93	3.69	15.42	8.67	0.19	6.22	13.06	2.74	2.26	0.47	0.12	785	1278	835	1563
1938 Eruption															
NYA0702-8	45.74	3.60	15.33	12.70	0.27	5.49	8.82	3.77	2.84	0.50	0.13	798	1071	835	1747
NYA0702-10	45.36	3.58	15.03	12.97	0.25	5.28	8.56	3.42	2.80	0.60	0.15	745	1643	812	1685
NYA0702-3	41.94	5.03	15.58	10.45	0.19	6.57	11.93	3.06	2.35	0.56	0.04	89	1664	728	1691
NYA0702-4	44.62	3.67	14.96	13.62	0.25	5.64	9.61	3.32	2.58	0.47	0.16	5212	105	53	1
1912 Eruption															
NYA0703	43.16	3.36	9.79	9.14	0.124	13.4	11.41	1.62	2.22	0.67	0.37	269	3670	1270	790

processes that influence inclusion composition, such as variations caused by pre-entrapment and post-entrapment crystallization.

[19] Our data show that most melt inclusions are more primitive than whole rock samples (Figure 2a), and the variations in melt inclusion compositions suggest fractional crystallization of olivine and potentially pyroxene. *Aoki et al.* [1985] attributed Nyamuragira whole rock major element variations to the fractionation of 30–40% olivine, clinopyroxene, plagioclase, and magnetite using a least squares mixing model. They determined that olivine was the first phase to crystallize and, therefore, we chose olivine-hosted melt inclusions to increase the likelihood of sampling primitive melt compositions. Within our data set, the highest MgO concentration (13 wt%) was found in the 1912 melt inclusion. However, the 1912 inclusion has similar K_2O and higher P_2O_5 concentrations compared to the more evolved 1986 and 2006 inclusions, suggesting that the 1912 inclusion does not represent a parental composition for the more evolved magmas. In addition, the 1912 inclusion has significantly higher S and Cl but lower F than most of the other inclusions, despite the similar K_2O values. These features suggest that the 1912 inclusion was derived from a different mantle source, and it may represent a more

Table 3. Corrected Melt Inclusion Major Elements and Volatiles

Sample	SiO_2	TiO_2	Al_2O_3	FeO_T	FeO	Fe_2O_3	MnO	MgO	CaO	Na_2O	K_2O	P_2O_5	H_2O (wt%)	CO_2 (ppm)	S (ppm)	Cl (ppm)	F (ppm)	Mg#	± olivine	Entrapment P (kbars)
2006 Eruption																				
NYA0705-1	44.04	3.37	15.00	11.74	8.28	3.85	0.19	5.56	11.26	3.18	2.07	0.54	1.36	892	2291	835	1555	54	1.2	0.82
NYA0705-4a	46.00	3.45	15.41	12.19	8.98	3.57	0.18	5.97	11.04	2.91	2.15	0.42	1.20	964	2284	802	1548	54	7.3	0.89
NYA0705-4b	45.98	3.51	15.30	12.42	8.87	3.95	0.17	5.88	11.27	2.68	2.10	0.44	1.25	700	2189	780	1503	54	2.8	0.71
NYA0705-5b	45.07	3.29	14.45	12.49	9.23	3.62	0.21	6.46	12.29	2.33	1.89	1.22	1.19	668	2281	810	1599	56	8	0.6
NYA0705-9	45.87	3.37	15.14	12.63	9.09	3.93	0.19	6.10	10.98	2.88	2.15	0.44	1.26	863	2278	826	1561	54	4.1	0.83
NYA0705-10a	45.81	3.64	15.16	12.07	8.64	3.81	0.19	5.81	11.37	2.99	2.12	0.55	1.27	937	2178	815	1572	55	3.2	0.88
NYA0705-10b	45.57	3.28	15.03	12.62	9.12	3.89	0.16	6.15	11.31	3.02	2.12	0.47	1.14	840	2241	822	1574	55	3.2	0.75
NYA0705-12a	45.65	3.51	15.39	12.46	8.94	3.91	0.22	5.94	10.36	3.34	2.31	0.55	1.24	470	2365	856	1605	54	4.8	0.52
NYA0705-12b	45.33	3.58	15.19	12.52	9.06	3.85	0.15	6.00	11.38	2.96	2.13	0.46	1.25	1862	2202	794	1568	54	3.6	1.47
NYA0705-11	46.91	3.50	15.98	12.02	8.61	3.79	0.21	5.84	10.14	2.12	2.52	0.49	1.24	1486	2150	786	1527	55	4.8	1.41
1986 Eruption																				
NYA0706-3a	48.32	3.29	16.88	11.42	8.10	3.69	0.23	4.61	8.92	1.99	3.57	0.56	1.35	1749	1978	965	2157	50	3.3	2.09
NYA0706-3b	47.05	3.63	16.21	12.17	8.63	3.93	0.21	4.90	11.72	3.14	1.89	0.47	1.34	1734	1525	987	2157	50	2	1.78
NYA0706-4	46.64	3.38	15.73	12.25	8.81	3.82	0.24	5.63	9.85	2.89	2.62	0.55	0.88	417	1296	864	1836	53	3.8	0.44
NYA0706-5	47.24	3.51	16.73	11.96	8.55	3.79	0.22	5.12	9.16	2.57	2.77	0.52	1.04	1743	1882	827	1837	52	3.8	1.78
NYA0706-6	46.24	3.40	16.22	12.27	8.77	3.89	0.20	5.27	12.71	2.54	1.97	0.33	1.06	350	1829	878	1519	52	3.2	0.42
NYA0706-7	46.33	3.44	15.56	12.16	8.76	3.78	0.22	6.01	9.66	3.18	2.74	0.47	0.62	383	1552	760	1799	55	4.2	0.34
NYA0706-10	46.83	4.19	16.39	11.12	8.07	3.39	0.25	4.79	10.60	2.52	2.68	0.36	0.97	1710	2081	933	1945	51	4.2	1.58
NYA0706-8	46.50	4.11	15.91	12.28	8.85	3.81	0.23	5.24	10.70	1.99	2.42	0.39	1.38	1164	1972	722	1850	51	4.3	1.24
1948 Eruption																				
NYA-07-1	46.35	4.10	16.04	13.12	8.76	4.84	0.22	3.61	8.90	4.04	2.92	0.57	0.05	91	964	770	1923	42	−10.9	0.08
NYA0701-3	44.38	3.48	15.69	11.54	7.77	4.19	0.28	3.72	9.84	4.71	2.77	0.48	0.16	ND	1085	739	1676	46	−4	ND
NYA0701-7	45.05	3.71	15.78	11.36	7.52	4.27	0.28	3.33	8.93	3.91	2.85	0.53	0.25	740	337	83	2	44	−5.6	0.51
NYA0701-15	46.45	2.94	19.81	11.11	7.14	4.41	0.25	2.97	10.01	3.87	2.72	0.44	0.26	900	1068	732	1858	43	−8.4	0.71
NYA0701-4	46.24	3.04	19.10	11.37	7.51	4.29	0.27	3.51	10.14	3.71	2.64	0.37	0.15	32	708	574	1422	45	−6	0.03
FTIR-Da	45.62	4.02	16.45	12.47	8.46	4.46	0.24	4.26	10.09	3.49	2.73	0.50	0.03	1473	1331	740	1759	47	−4.1	1.07
FTIR-Db	45.89	4.00	16.45	11.50	7.68	4.25	0.22	3.89	11.86	3.61	2.65	0.53	0.17	922	317	200	92	47	−3.7	0.72
FTIR-G	45.27	3.68	16.08	11.57	8.15	3.80	0.18	6.71	9.95	3.32	2.63	0.48	0.17	923	1325	809	1550	59	−5.5	0.65
FTIR-B	44.56	3.73	16.60	12.12	8.30	4.25	0.25	4.77	10.73	3.90	2.68	0.51	0.08	79	1237	755	1602	51	10.9	0.05
FTIR-E	45.08	4.04	17.23	11.38	7.47	4.34	0.17	3.75	14.52	3.58	2.54	0.49	0.17	ND	1410	767	1616	47	−10.9	ND
FTIR-Ca	45.77	3.67	15.34	12.12	8.62	3.89	0.19	7.38	12.99	2.72	2.25	0.47	0.14	664	1302	851	1594	60	−7.3	0.5
1938 Eruption																				
NYA0702-8	45.77	3.43	14.62	13.11	9.47	4.04	0.26	7.57	8.41	3.59	2.71	0.47	0.12	651	1076	919	2183	59	10.9	0.54
NYA0702-10	46.48	3.74	15.66	13.08	9.02	4.51	0.27	4.69	8.92	3.56	2.92	0.62	0.12	789	1076	839	1756	48	−10.9	0.66
NYA0702-3	42.90	5.16	15.98	11.99	8.38	4.01	0.20	6.60	12.24	3.14	2.41	0.57	0.16	958	1101	715	2207	58	4	0.5
NYA0702-4	44.79	3.50	14.06	12.27	8.88	3.77	0.25	7.88	9.15	3.17	2.45	0.45	0.13	759	1696	741	1722	61	6.4	0.53
1912 Eruption																				
NYA0703	45.36	3.57	10.65	12.02	8.39	4.03	0.16	13.30	12.15	1.64	2.44	0.70	0.37	269	3671	1323	795	74	1.8	0.12

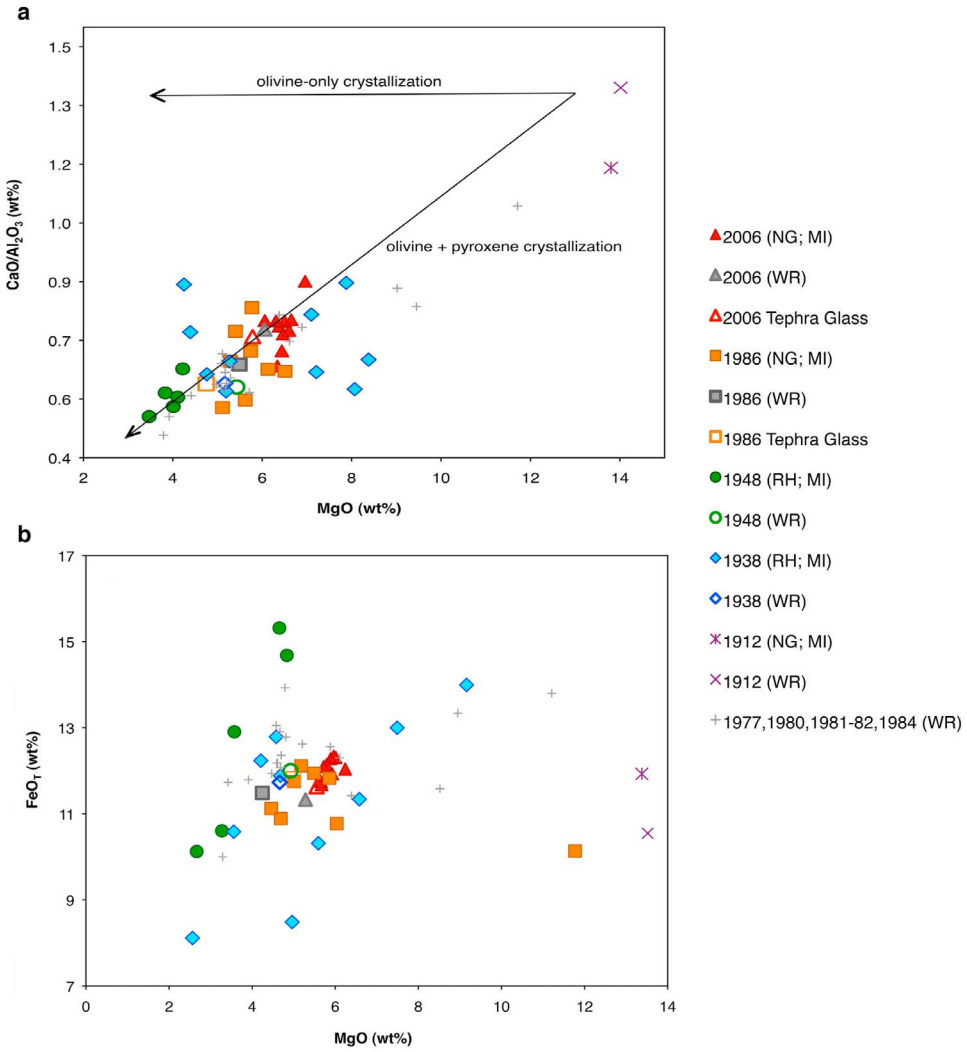

Figure 2. For all variations diagrams, melt inclusions are "MI," naturally glassy inclusions are "NG," rehomogenized inclusions are "RH," and whole rock is "WR." The 1984 WR data are from *Katabarwa et al.* [1986] and the 1977, 1980, and 1981–82 WR data are from *Aoki et al.* [1985]. (a) MgO versus CaO/Al_2O_3 data suggest olivine + clinopyroxene crystallization; (b) MgO versus FeO_T data suggest Fe loss and gain for inclusions with FeO_T concentrations that fall outside the 11–13 wt% FeO_T range set by the majority of our melt inclusion, tephra glass, and whole rock data.

volatile-rich magma composition in the Nyamuragira system. The fact that the 1912 Rumoka eruption was unusually explosive compared to other Nyamuragira eruptions also supports a higher volatile concentration in the 1912 magma. The high S content (3700 ppm), in particular, suggests that some Nyamuragira magmas may initially be very S-rich at depth, as implied by the large SO_2 emissions measured from its eruptions. The Mg# (100 * MgO/(FeO + MgO)) of host olivines from our data set range from 71 to 84, and melt inclusions range from Mg# 42 to 61, with the exception of the 1912 inclusion (olivine Mg # = 90; melt inclusion Mg # = 74).

[20] Most corrected melt inclusion FeO_T data fall within a distinct range of values that are similar to whole rock and matrix glass compositions. Deviations from this trend suggest post-entrapment diffusion of Fe and, in fact, 11 out of 34 inclusions have values that indicate potential Fe loss or gain (Figure 2b). Data from five 1938 and four 1948 reheated inclusions, and two 1986 naturally glassy inclusions, were significantly above or below the MgO versus FeO_T range set by the remainder of the melt inclusion data, as well as the matrix glass and the majority of the whole rock data. If a primary (co-entrapped) titanomagnetite crystal had been present within the devitrified inclusions and sub-

sequently melted during reheating, this addition could explain the anomalously high FeO_T data [*Rowe et al.*, 2007]. Anomalously low FeO_T in some of the reheated and naturally glassy inclusions, however, suggests that Fe diffused out of the inclusion [*Danyushevsky et al.*, 2000]. *Gaetani and Watson* [2000] have shown that various amounts of Fe and Mg diffusion can occur between the melt inclusion and the olivine host while the melt inclusion is still within the magma reservoir. We addressed this variation by adjusting the original FeO_T values of the anomalous data points to 12 wt% FeO_T [e.g., *Danyushevsky et al.*, 2000; *Johnson et al.*, 2010]. This value fell within the range of FeO_T concentrations (11–13 wt%) that defined the majority of our data set. New PEC corrections were then carried out only for the inclusions that fell outside of the 11–13 wt% FeO_T range.

4.2. Melt Inclusion Volatile Concentrations

[21] The naturally glassy melt inclusions from the 1986 and 2006 eruptions generally have the highest H_2O and CO_2 concentrations (Figure 3a and Table 3). H_2O contents of the 1986 and 2006 melt inclusions range from 0.6 to 1.4 wt %, and CO_2 contents range from 350 to 1900 ppm. These data are higher than MORB H_2O values (0.1–0.3 wt%), but overlap the typical range for E-MORB values (0.3–1.0 wt% [e.g., *Dixon et al.*, 1995]). Our inclusions contain significantly higher CO_2 concentrations than typical MORB (<350 ppm in both MORB inclusions and glassy pillow rims [e.g., *Saal et al.*, 2002; *le Roux et al.*, 2006]). The 1912, 1938 and 1948 samples have CO_2 concentrations ranging between 30 and 1000 ppm, but H_2O contents are significantly lower (0.03–0.4 wt %) than inclusions from the tephra samples. Other than rehomogenization causing potential H_2O loss, the low H_2O concentrations observed in the 1938 and 1948 samples could have resulted from the H diffusion that readily occurs during slow cooling of lava flows (Figure 3b) [e.g., *Hauri*, 2002; *Metrich and Wallace*, 2008].

[22] A high CO_2 content melt inclusion should have lost minimal amounts of S, owing to the lower solubility of CO_2 relative to S. Based on the observation of relatively uniform S concentrations over a range of CO_2 values, we suggest little pre-eruptive S degassing for the 2006 eruption (Figure 3c). The primary CO_2 contents of our Nyamuragira magmas are unknown, although there is evidence supporting alkalic magmas being initially CO_2-rich [*Spera and Bergman*, 1980; *Dixon*, 1997]. Primary CO_2 concentrations in non-alkalic magmas at Kilauea (Hawaii) and the Michoacan-Guanajuato Volcanic Field (Mexico) are estimated to be ~0.6–0.7 wt%; melt inclusions trapped at shallow depths in these systems record significant CO_2 loss at upper crustal pressures [*Gerlach and Graeber*, 1985; *Wallace*, 2005; *Johnson et al.*, 2010]. If we assume that Nyamuragira magmas start off with a higher CO_2 content than the Kilauea and Michoacan-Guanajuato systems, our data also suggest strong degassing of CO_2 prior to entrapment. In addition to CO_2, degassing of S could have occurred prior to inclusion entrapment as the magma ascended and cooled, particularly for the 1938, 1948, and 1986 inclusions (Figure 3c).

[23] Sulfur concentrations of the 2006 sample show little variation (2100–2400 ppm), whereas the 1986 S data show slightly more variability (1300–2000 ppm) and suggest some S loss. A clear degassing pattern in the 1938 and 1948 data is difficult to see due to scatter. The 1938 and 1948 samples with 300–1700 and 300–1000 ppm S, respectively, also show wider variation than the 2006 sample. The 1912 melt inclusion has the highest S concentration (~3700 ppm). The range of Nyamuragira S concentrations are comparable to values reported for melt inclusions in other alkaline systems. The Nyamuragira data lie between Etna (alkali basalt), Kilauea (alkali basalt), Vulcano (shoshonitic basalt), and Mt. Cameroon (basanite) samples, which range in S concentration from 1000 to 3500 ppm (Figure 4) [*Metrich and Clocchiatti*, 1996; *Spilliaert et al.*, 2006; *Coombs et al.*, 2006; *Suh et al.*, 2008]. Melt inclusions from cinder cones around the flanks of Colima volcano (Mexico; basanite, minette) contain the largest S concentrations (~5000 ppm) reported thus far. In comparison with MORB S concentrations (1300–1700 ppm S; *PetDB*), the 1938 and 1948 data are low, whereas the 1986 and 2006 data are relatively high, and the 1912 S concentration (3700 ppm) is well above the range of MORB values.

[24] Chlorine concentrations (800–1300 ppm) are significantly higher than MORB values (<150 ppm [*Michael and Schilling*, 1989]), but are within the range of other alkali basalt and basanite values from Italy, Hawaii, Mt. Cameroon, and Mexico (100–2500 ppm [*Spilliaert et al.*, 2006; *Coombs et al.*, 2006; *Suh et al.*, 2008; *Vigouroux et al.*, 2008]). Fluorine concentrations (92–2200 ppm) overlap MORB (300–840 ppm; *PetDB*]) and Mt. Cameroon (1530–1982 ppm; basanite [*Suh et al.*, 2008]) values. Two exceptions of anomalously low Cl and F values are found in the 1938 and 1948 samples (Table 3). We note that the 1938 and 1948

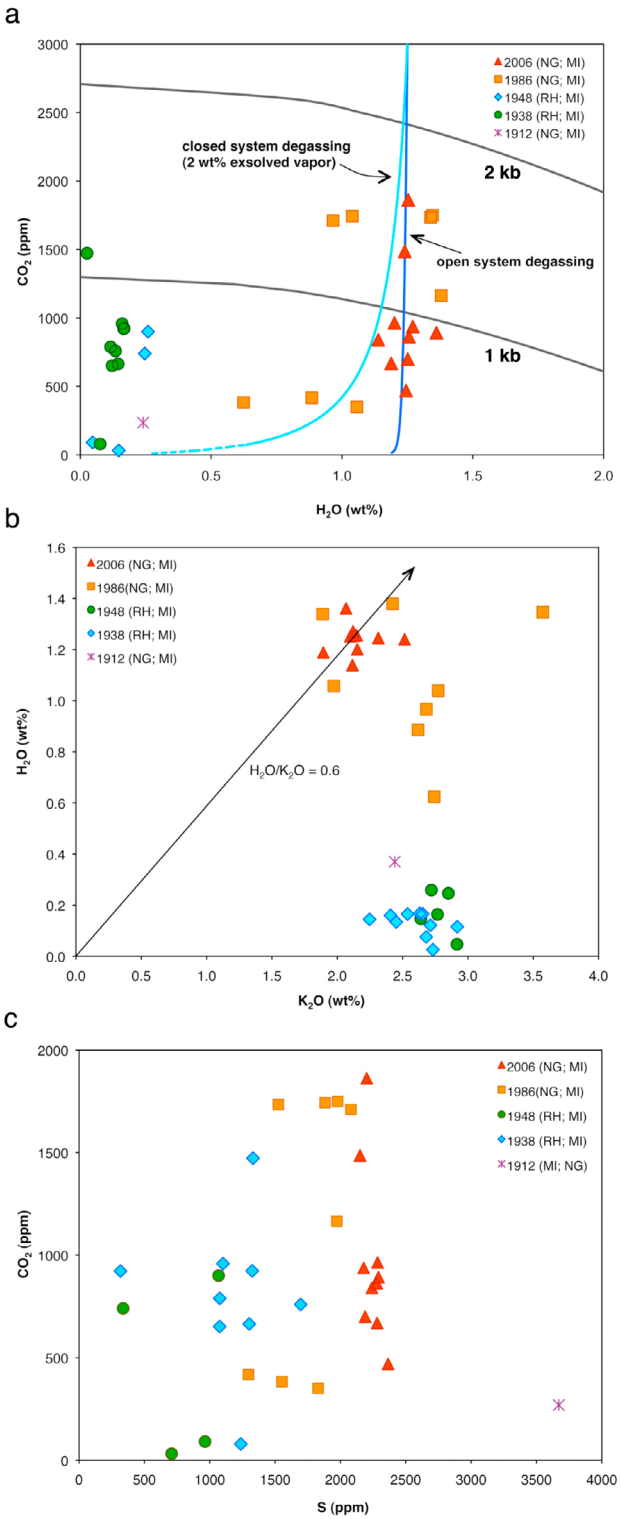

Figure 3. (a) Melt inclusion entrapment pressures calculated from Nyamuragira H_2O and CO_2 data allow an assessment of degassing with decompression. Assuming vapor saturation, these entrapment pressures, degassing trends, and isobars were calculated with VolatileCalc [*Newman and Lowenstern*, 2002]. We modeled the degassing trends for the tephra samples only (1986 and 2006), due to likely H loss from lava flow samples (1938 and 1948). The 2006 data are best fit by an open system trend, whereas the 1986 data are best fit by a closed system trend with 2% exsolved vapor coexisting in the melt; (b) S versus CO_2 data suggest little S degassing with ascent; (c) K_2O versus H_2O suggest that some 1986 samples trapped melts degassed of H_2O.

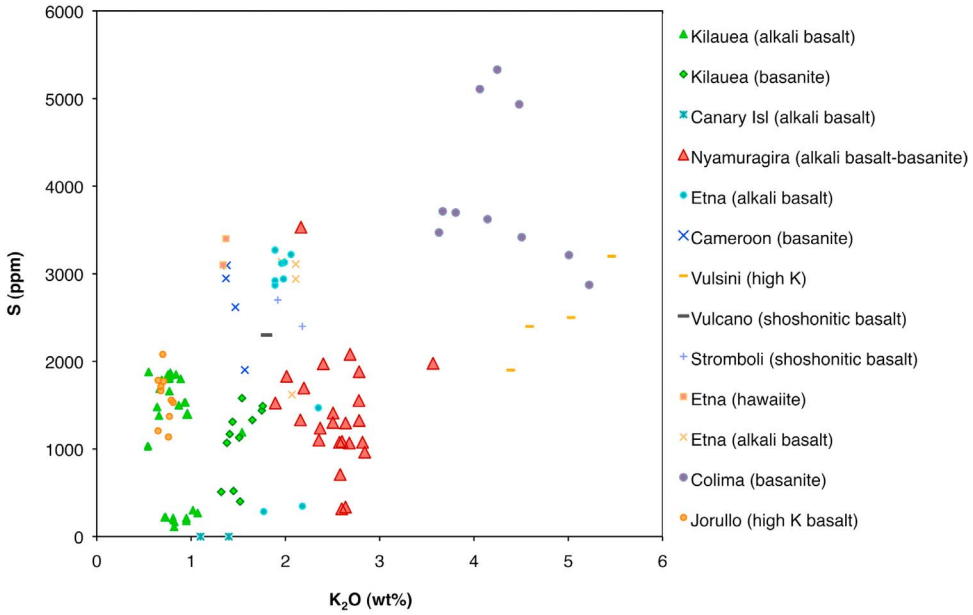

Figure 4. K_2O versus S for Nyamuragira melt inclusion data, along with global S melt inclusion data from: *Vigouroux et al.* [2008] (Colima); *Spilliaert et al.* [2006] (Etna); *Johnson et al.* [2008] (Jorullo); *Coombs et al.* [2006] (Kilauea); *Metrich et al.* [2004] (Etna); *Suh et al.* [2008] (Cameroon); *Gurenko et al.* [2001] (Canary Islands); *Metrich and Clocchiatti* [1996] (Vulsini; Volcano and Stromboli; Etna).

samples with the lowest Cl and F also have the lowest S in the data set, suggesting that these samples may have suffered extensive degassing.

5. Discussion

5.1. Melt Inclusion Entrapment Depths and Volatile Degassing

[25] The volatile contents of Nyamuragira melt inclusions suggest that the melts have undergone variable extents of degassing. Interpreting this variation requires an assessment of the magmatic processes that occur throughout magma storage, ascent, and eruption. As magma ascends, decompression can induce both degassing and crystallization [e.g., *Sisson and Layne*, 1993; *Roggensack*, 2001; *Couch et al.*, 2003; *Blundy and Cashman*, 2005]. The following discussion will consider the degassing history of melts from Nyamuragira, focusing primarily on naturally glassy (rather than re-homogenized) melt inclusions from the 1912, 1986, and 2006 eruptions. We consider these samples to best represent pre-eruptive Nyamuragira magma compositions and hence we use them to estimate syn-eruptive SO_2 degassing for comparison with satellite-based SO_2 measurements.

[26] Estimates of melt inclusion entrapment depths using H_2O and CO_2 data allow crystallization and degassing to be placed within the context of magma ascent and storage. Water and CO_2 concentrations can be used to infer the depth at which melt inclusions are trapped based on experimentally determined solubility relationships and assuming that the melts were vapor saturated when they were trapped. Entrapment pressures (Table 3) and degassing paths are calculated using VolatileCalc [*Newman and Lowenstern*, 2002] (Figure 3a).

[27] The 1986 and 2006 melt inclusion data indicate entrapment over a range of pressures from 1-~1.7 kb (~3–5 km). This is consistent with magma chamber depth estimates inferred from seismic investigations, which range from 3–7 km [*Hamaguchi*, 1983]. The 2006 data define a trend that is best explained by open system degassing, whereby volatiles can escape from the melt after exsolution. The 1986 data show more scatter and do not define any coherent degassing path. Some of the variation could be explained by closed system degassing with excess exsolved gas (see Figure 3a), but other more complex processes like open system gas fluxing [e.g., *Spilliaert et al.*, 2006; *Johnson et al.*, 2008] could also account for the scatter. For both the 1986 and 2006 eruptions, we used the highest H_2O and CO_2 values in the data set (presumably the deepest melts) to represent initial magma compositions. The 2006 data suggest that, as the magma decompresses over the ~3–5 km

depth range, CO_2 exsolves while H_2O remains dissolved in the melt. Our data agree well with modeling studies for alkalic systems, which show that CO_2 exsolves at depths ranging from ~3–6 km while H_2O does not exsolve until ~1 km depth [*Dixon*, 1997].

[28] *Wallace and Anderson* [1998] evaluated melt inclusion H_2O and K_2O data to assess the effects of magma degassing on melt inclusion compositions prior to entrapment. On a plot of K_2O versus H_2O, an H_2O/K_2O ratio (1.3) was established from the least degassed data, and all data below this line were interpreted as having degassed variable amounts of H_2O. For our samples, if we assume a constant H_2O/K_2O ratio (0.6) for the initial undegassed magma (based on a line projected from the origin to the highest H_2O values in our data set), the 1986 and 2006 data points that fall below this line are likely to have undergone H_2O degassing prior to entrapment (Figure 3c). The low H_2O data from the reheated inclusions are, as discussed above, likely due to either H-loss by diffusion in the lava or possibly by the reheating process itself.

[29] From S, Cl, and F concentrations plotted against Mg# (Figure 5), we find that the single 1912 inclusion is exceptionally primitive and S and Cl rich, whereas the 1986 and 2006 inclusions are more evolved but still relatively undegassed compared to the 1938 and 1948 samples. Sulfur concentrations decrease with decreasing Mg# for the 1938, 1948, and 1986 eruptions (Figure 5a). This trend is consistent with simultaneous fractional crystallization and degassing. Excluding the 1912 inclusion, Cl and F data neither decrease nor increase with decreasing Mg# (Figures 5b and 5c, respectively). Furthermore, residual Cl and F measured in the tephra glasses (800 and 1300 ppm, respectively, for the 2006 sample and 900 and 1700 ppm, respectively, for the 1986 sample) support the assumption that Cl and F do not degas significantly prior to or even during eruption. The 1912 sample has lower F and CO_2 concentrations than the rest of the data set.

5.2. Sulfur Solubility in Nyamuragira Magma

[30] In order to make robust estimates of primary melt S concentrations, we need to evaluate S solubility and determine whether Nyamuragira melts have been influenced by variable oxidation conditions. More specifically, could primary Nyamuragira magmas contain enough S to account for what is observed in SO_2 emissions? Sulfur concentrations measured in MORB glasses are typically controlled by immiscible sulfide liquid saturation [*Mathez*, 1976; *Wallace and Carmichael*, 1992]. The positive correlation between FeO_T and S in basaltic glasses with relatively low oxygen fugacities is caused by the effect of FeO on S solubility. In contrast, magmas that have oxygen fugacities higher than NNO contain a substantial proportion of sulfate, which makes the total S solubility much higher than for MORB [e.g., *Metrich and Wallace*, 2008]. Some of our Nyamuragira data fall within the range of MORB values that are controlled by this sulfide-saturation field, with other points plotting both below and above the field (Figure 6). Thermodynamic modeling as described by *Wallace and Carmichael* [1992] can be used to estimate S solubilities at fO_2 < NNO and 1150°C for Nyamuragira magmas (Figure 6). The results require that Nyamuragira data lying above the NNO solubility curve represent inclusions with fO_2 values that were higher than NNO, whereas lower values may represent melts that originally contained a higher S concentration but have degassed S prior to inclusion entrapment. An interesting outlier in our data is the 1912 inclusion, which has significantly higher S than the rest of the data set for a given FeO_T. We cannot draw solid conclusions with this one data point, but it suggests that magma with even higher fO_2 may exist in the Nyamuragira system. Our S data indicate that Nyamuragira magmas commonly have a higher fO_2 than NNO, resulting in relatively high initial S contents.

[31] We acknowledge the fact that the melt inclusions may not record primary volatile contents of the melt, as some volatile loss by degassing prior to entrapment may have occurred, evidenced by the solubility calculations and discussion of variations in H_2O/K_2O. The 1986 and 2006 melt inclusion compositions are also more evolved than the primitive 1912 inclusion composition, and S could therefore have been partially degassed from the melts during cooling and differentiation, which could explain the lower S values found in many inclusions.

5.3. Comparison Between Satellite-Based SO_2 Emissions, Lava Volumes, and Estimated SO_2 Emissions From Melt Inclusion Data

[32] Nyamuragira emits large amounts of SO_2 (up to 1.7 Mt/day; 1981 eruption) compared to both arc and non-arc volcanic eruptions (Figure 7), but the source of the SO_2 emissions (e.g., syn-eruptive S release from melt or release of a pre-eruptive vapor phase)

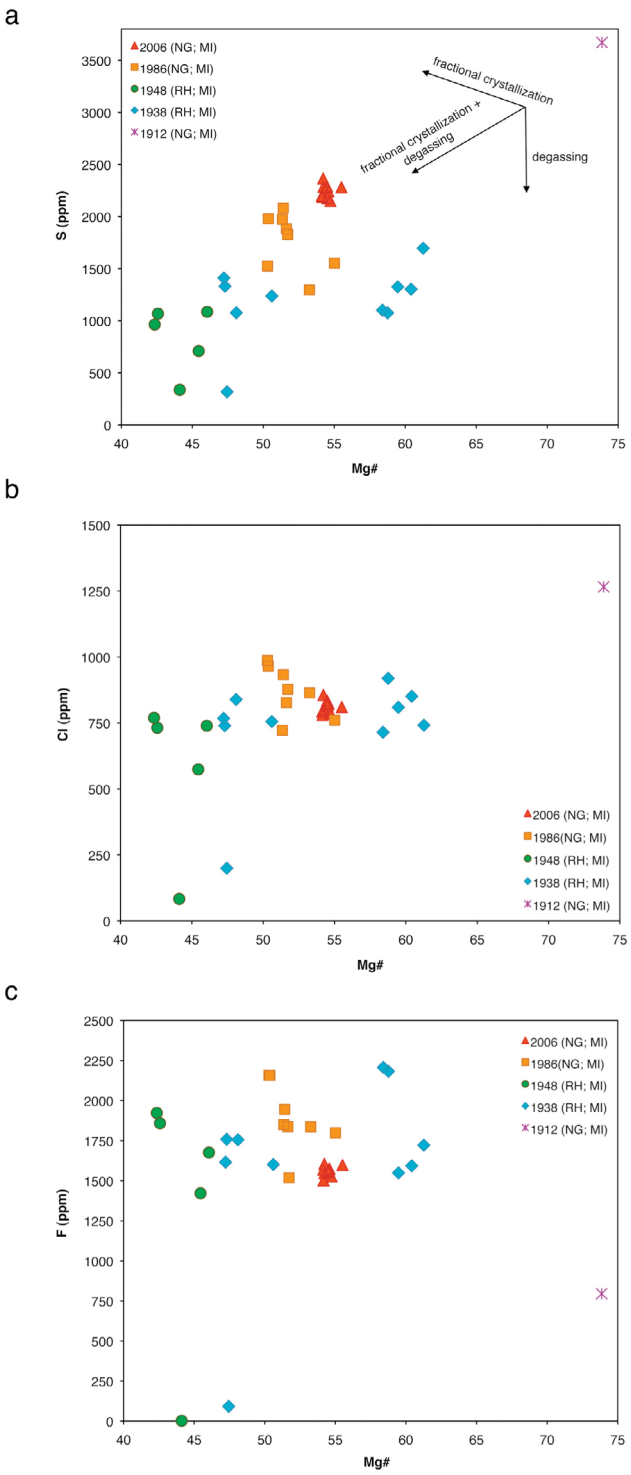

Figure 5. (a) S versus Mg#; (b) Cl versus Mg#; (c) F versus Mg#. The 1912 inclusion is exceptionally primitive and S and Cl rich, whereas the 1986 and 2006 inclusions are more evolved but still relatively undegassed compared to the 1938 and 1948 samples. The S versus Mg# trend is consistent with simultaneous fractional crystallization and degassing. Cl and F neither decrease nor increase with decreasing Mg# and residual Cl and F measured in the tephra glasses (800 and 1300 ppm, respectively, for the 2006 sample and 900 and 1700 ppm, respectively, for the 1986 sample) suggest that Cl and F do not degas significantly prior to or even during eruption.

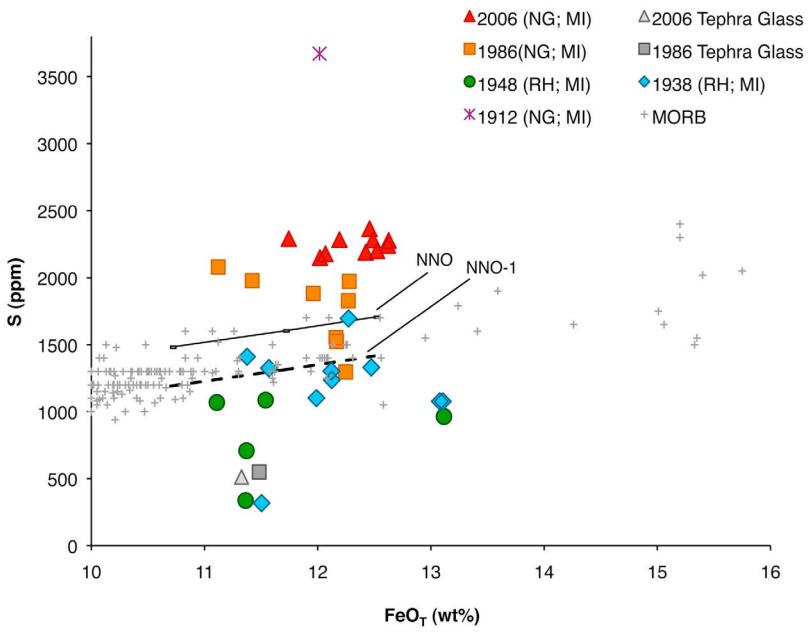

Figure 6. S versus FeO_T data for Nyamuragira melt inclusions and tephra glasses compared to MORB glasses. The relatively high S contents of some Nyamuragira melt inclusions require fO_2 values > NNO. The NNO and NNO-1 lines were calculated using the method of *Wallace and Carmichael* [1992], modified to incorporate the temperature dependence of *Mavrogenes and O'Neill* [1999], for Nyamuragira magmas with a range of FeO_T contents (11–13 wt%) at 1150°C and NNO. The S solubility model is not calibrated for fO_2 higher than NNO.

and the mechanisms of S release during eruptions are poorly understood. An important aim of our study, therefore, is to compare Nyamuragira SO_2 emission estimates based on satellite data (TOMS and OMI measurements) to estimates of SO_2 released based on melt inclusion data and lava flow volume estimates (Figure 7). We estimated the total amount of SO_2 released from Nyamuragira for the

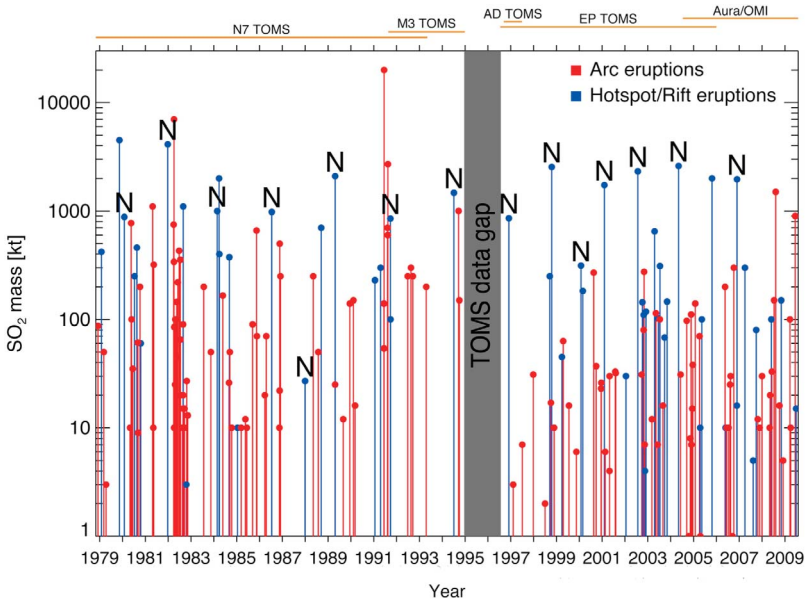

Figure 7. Global volcanic SO_2 emissions (kt) measured by the Total Ozone Mapping Spectrometer (TOMS) sensors and the Ozone Monitoring Instrument (OMI) since 1978. The blue lines represent individual non-arc eruptions and the red lines represent individual arc eruptions that detected by TOMS and/or OMI. Nyamuragira eruptions are labeled with an "N." Since 1980, Nyamuragira has been one of the most prolific sources of volcanic SO_2.

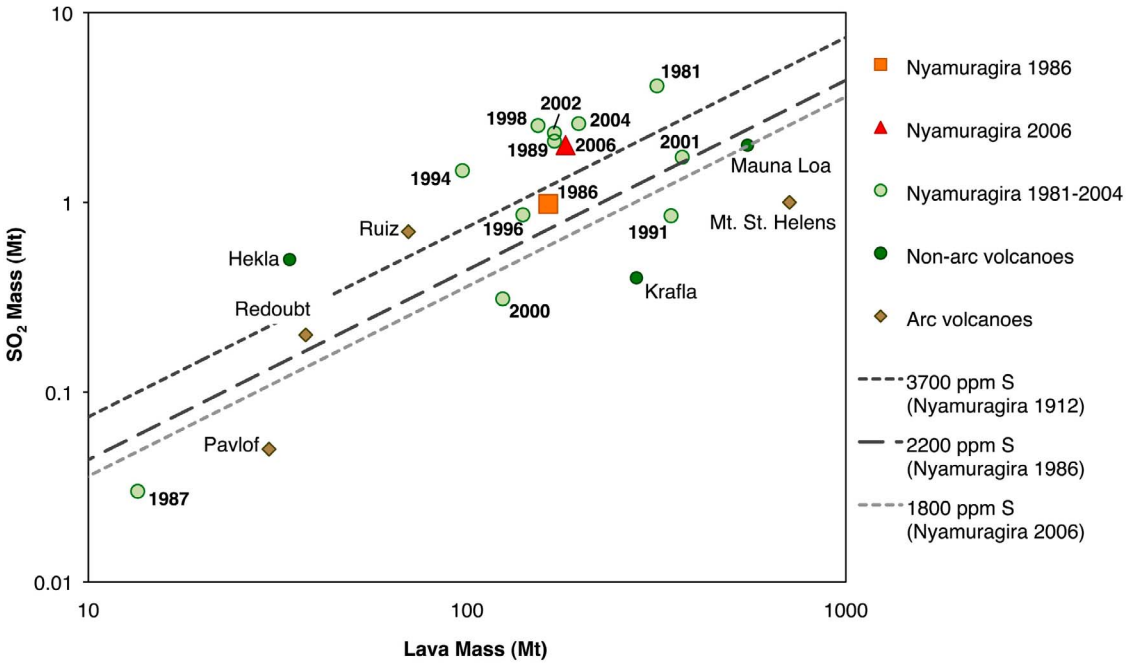

Figure 8. Lava and SO_2 mass (Mt) measured by satellite remote sensing methods. The diagonal lines show the amounts of SO_2 released by syn-eruptive degassing based on concentrations of S we measured in melt inclusions from the 1912, 1986 and 2006 samples. The 1986 and 2006 eruptions are the only Nyamuragira eruptions with both melt inclusion volatile data and remotely sensed SO_2 measurements available. The satellite SO_2 measurements for the 1986 and 2006 eruptions lie above the lines representing the highest S concentrations, which imply that a mechanism other than syn-eruptive degassing occurred for both eruptions. Other Nyamuragira eruptions for which we have SO_2 emission estimates also plot above the highest measured S concentrations.

1986 and 2006 events using the petrologic method, whereby S contents in melt inclusions are scaled to erupted lava volumes. Lava volumes were calculated using satellite-based lava flow maps and published lava flow thicknesses (1986 = 0.063 km^3; 2006 = 0.070 km^3 (E. M. Head et al., manuscript in preparation, 2011)). The resulting petrologic estimates are 0.04 Mt SO_2 for the 1986 eruption and 0.06 Mt SO_2 for the 2006 eruption. These results are significantly smaller than the SO_2 emissions measured through satellite-based methods for the same eruptions (~1 Mt for 1986 [*Bluth and Carn*, 2008] and ~2 Mt for 2006). Measured SO_2 emissions for a number of recent Nyamuragira eruptions (1980–2006) compared to petrologic estimates based on the melt inclusion data further illustrate this point (Figure 8).

[33] Errors associated with the satellite measurements are ±30% and the petrologic method has a combined error (melt inclusion S measurements and lava volume calculations) of ±22%. Using the highest melt inclusion S concentration we measured (3700 ppm; 1912) still does not resolve the discrepancy, as the satellite-based SO_2 measurements require as much as 5000 ppm S or more to explain the SO_2 emissions by syn-eruptive degassing. Although magmatic S concentrations up to 5000 ppm have been measured in melt inclusions from potassic magmas on the flanks of Colima volcano (Mexico [*Vigouroux et al.*, 2008]), there is no evidence in the Nyamuragira melt inclusions that such high concentrations are present in primitive melts.

5.4. Degassing Mechanisms at Nyamuragira

[34] The origin of excess S emissions at Nyamuragira can be assessed through the examination of degassing mechanisms. As the degassing process can strongly influence eruption style, we summarize Nyamuragira's recent eruptive activity and then evaluate two different degassing models that are consistent with our observations.

[35] Nyamuragira eruptions typically begin with fire fountaining, a gas-rich jet that propels hot lava from the vent(s) to heights of several hundred meters [*Swanson et al.*, 1979]. This eruption style was first documented at Kilauea (Hawaii) and is, therefore,

often termed "Hawaiian." Initial fountain heights at Nyamuragira are ~200 m and, as eruptions progress, these fountain heights diminish until the end of the eruption; during the fire fountaining phases SO_2 emissions also start high and wane as the eruption proceeds [*Bluth and Carn*, 2008]. During the middle to late phase of some eruptions, renewed fire fountaining occurs, although fountain heights are reduced compared to the initial activity, and/or Strombolian-style eruptions are observed (Smithsonian Institution, monthly reports, 1971–2010), consisting of large gas slugs bursting at the vent [*Wilson*, 1980].

[36] For the 2006 Nyamuragira eruption, initial fire fountain heights were over 300 m, whereas the 1986 fire fountains reached a maximum height of 200–250 m [*Smithsonian Institution*, 2006]. Satellite-based SO_2 emissions from the 2006 eruption (~2 Mt) are significantly larger than those from the 1986 eruption (~1 Mt), and there is a larger excess S component observed for the 2006 eruption compared to the 1986 eruption. The gas plume associated with the 2006 eruption plume reached the tropopause and could be tracked for almost a week by satellites, whereas maximum plume altitudes during the 1986 eruption were ~9 km [*Bluth and Carn*, 2008]. Higher fire fountain and plume heights, along with larger SO_2 emissions suggests that the 2006 eruption was more energetic than the 1986 eruption [*Wilson*, 1980; *Wilson and Head*, 1981; *Parfitt and Wilson*, 1999].

[37] Two models of degassing can be considered to explain the eruptive behavior at Nyamuragira. First, the collapsing foam model (CF [*Vergniolle and Jaupart*, 1990]) where degassing of basaltic magma results in exsolved gas bubbles rising to the roof of a reservoir, creating a foam layer. When this foam layer reaches a critical thickness, it collapses and eruption occurs. If the collapse is instantaneous, Hawaiian-style activity results; but if there is sufficient time for bubbles to coalescence within the foam, a Strombolian eruption results. Second, the rise speed dependent model (RSD [*Wilson*, 1980; *Wilson and Head*, 1981]) where the speed at which magma ascends controls the style of eruption instead of a foam collapse. If the rise speed is high, the bubbles move with the magma, allowing a homogeneous two-phase flow until fragmentation at the surface (i.e., Hawaiian-style eruption). A slower magma rise speed would allow the bubbles to rise faster than the magma and coalesce, creating a Strombolian eruption. A decrease in gas content would not cause the style to change from Hawaiian to Strombolian, as has been postulated for the CF model. Instead, a decrease in gas content with similar rise speeds would produce an effusive lava flow regime, which has been observed at basaltic volcanoes such as Kilauea and Nyamuragira.

[38] In the first case, we determine whether the accumulation of a foam layer is possible at Nyamuragira. Based on gas solubility behavior for alkaline magmas, CO_2 would have degassed to some extent during ascent to the magma reservoir at 3–7 km [*Dixon*, 1997]. Our melt inclusion data show that SO_2 degassing continued in the magma chamber along with fractional crystallization. Hence, accumulation of exsolved volatiles could have occurred in the magma reservoir prior to eruption. We suggest that a foam layer is plausible and that the CF model could explain fragmentation processes (eruption styles) associated with Nyamuragira degassing and the large excess SO_2 emissions during the fire fountain phases. In the second case, the RSD model could also explain the Hawaiian fire fountaining, Strombolian activity, and transitions between the two styles observed at Nyamuragira. As evidenced by our melt inclusion data, the 2006 magma did not contain significantly higher volatile concentrations than the 1986 magma, although we recognize that variable extents of degassing could have occurred prior to melt inclusion entrapment for either eruption. However, if both magmas had the same initial gas content, an explanation for the more energetic 2006 eruption, as well as the style transitions for both eruptions, could lie in differences in magma rise speeds rather than accumulation and collapse of a foam. A difference in the timescales of gas accumulation might have also influenced the eruption styles, although there were similar repose periods prior to the 2006 (29 months) and 1986 (28 months) eruptions.

[39] Both models address the fact that exsolved gas is propelled to the surface, often with little associated erupted magma. Reconciling the large Nyamuragira SO_2 emissions and disproportionate lava volumes, it is possible that some magma is degassing but not erupting. This degassed magma would then sink back into the system [*Allard et al.*, 1994; *Allard*, 1997]. We evaluated the amount of unerupted magma that would have to degas in order to explain the apparent excess SO_2 emissions. The 1986 and 2006 eruptions would have required degassing of ~1 km^3 and >2 km^3 of unerupted magma, respectively.

[40] In order to further constrain the application of these models to Nyamuragira activity, additional geochemical data sets are needed. In addition, the role of passive degassing in the system between

eruptions is unclear as ground-based measurements at Nyamuragira were not made due to political unrest. These data would allow a better assessment of the volatile budget at Nyamuragira. Gas composition data from techniques such as ground-based Fourier-Transform IR (FTIR) spectroscopy would be particularly useful for evaluating the degassing mechanisms during eruptions [e.g., *Allard et al.*, 2005; *Sawyer et al.*, 2008]. If a foam layer exists at Nyamuragira, the gases would have time to equilibrate with the melt, which would be reflected in volcanic gas ratios. For example, the CO_2/SO_2 and S/Cl ratios from FTIR measurements of fire fountaining from Etna (Italy) were shown to be higher than typical Etnean emissions. The ratios indicated exsolution and storage of CO_2 and SO_2 at depth, suggesting gas accumulation. A lower CO_2/SO_2 ratio would be indicative of syn-eruptive degassing of CO_2 and SO_2 [*Allard et al.*, 2005].

6. Conclusions

[41] New volatile data from Nyamuragira melt inclusions indicate inclusion entrapment over a range of pressures (vapor saturation pressures) from <1.0–1.7 kbar (~0.1–5 km), where the greater depths inferred agree with seismically determined estimates of magma storage depth. Nyamuragira melt inclusion volatile contents show evidence of variable extents of shallow degassing, which occurred together with crystallization. The 1986 and 2006 tephra samples yielded volatile concentrations that best represent initial values for Nyamuragira magmas. For the 1986 and 2006 eruptions, S concentrations ranged from 1300 to 2400 ppm, H_2O from 0.6 to 1.4 wt%, CO_2 from 350 to 1900 ppm, Cl from 720 to 990 ppm, and F from 1500 to 2200 ppm. The relatively high S contents of some Nyamuragira melt inclusions require higher-fO_2 values (>NNO) than MORB. Based on the melt inclusion data, the total SO_2 emissions for the 1986 and 2006 eruptions that could be produced by syn-eruptive degassing are 0.04 and 0.06 Mt, respectively, which is significantly less than satellite-derived estimates (~1 Mt for 1986 and ~2 Mt for 2006). Even when taking into account errors on the SO_2 emissions and melt inclusion S measurements, the magnitude of this discrepancy suggests an additional source of S for both eruptions. Variable pre-eruption gas loss, as inferred from the melt inclusion data, is consistent with a model of shallow degassing and gas accumulation, although the rise speed of the magma could also be influencing degassing and eruptive behavior at Nyamuragira. Ground-based gas composition measurements have not been possible to date due to the political climate of the region, but we stress the need for this type of data to further constrain Nyamuragira's degassing mechanisms.

Acknowledgments

[42] We dedicate this paper to Jim Luhr, who began this research endeavor with us, contributing greatly until his untimely death just a year into the project. Funding for this work was provided by NSF (grant EAR 0910795 (to SAC) and grant EAR 0646694 (to AMS)), as well as the National Geographic Society (grant 7698-04 (to SAC)). We are grateful for the assistance of Dario Tedesco, the late Jacques Durieux, the Goma Volcano Observatory staff, and the UNOPS with D.R. Congo fieldwork. We thank John Donovan for assistance with EMPA analysis at UO, Nobu Shimizu and Andrey Gurenko for assistance with SIMS analysis at WHOI, and Nilanjan Chatterjee for assistance with EMPA analysis at MIT. We would also like to thank Tyrone Rooney and an anonymous reviewer for thoughtful reviews that greatly improved the manuscript.

References

Allard, P. (1997), Endogenous magma degassing and storage at Mount Etna, *Geophys. Res. Lett.*, *24*(17), 2219–2222, doi:10.1029/97GL02101.

Allard, P., J. Carbonnelle, N. Metrich, H. Loyer, and P. Zettwoog (1994), Sulphur output and magma degassing budget of Stromboli volcano, *Nature*, *368*, 326–330, doi:10.1038/368326a0.

Allard, P., M. Burton, and F. Mure (2005), Spectroscopic evidence for a lava fountain driven by previously accumulated magmatic gas, *Nature*, *433*, 407–410, doi:10.1038/nature03246.

Anderson, A. T. (1974), Evidence for a picritic, volatile-rich magma beneath Mt. Shasta, California, *J. Petrol.*, *15*, 243–267.

Aoki, K., and T. Yoshida (1983), Petrological and geochemical studies on the 1981–1982 lava from Nyamuragira volcano, in *Volcanoes Nyiragongo and Nyamuragira: Geophysical Aspects*, edited by H. Hamaguchi, pp. 91–96, Tohoku Univ., Sendai, Japan.

Aoki, K., T. Yoshida, K. Yusa, and Y. Nakamura (1985), Petrology and gochemistry of the Nyamuragira Volcano, Zaire, *J. Volcanol. Geotherm. Res.*, *25*, 1–28, doi:10.1016/0377-0273(85)90002-2.

Blundy, J., and K. Cashman (2005), Rapid decompression-driven crystallization recorded by melt inclusions from Mount St. Helens volcano, *Geology*, *33*, 793–796, doi:10.1130/G21668.1.

Bluth, G. J. S., and S. A. Carn (2008), Exceptional sulfur degassing from Nyamuragira volcano, 1979–2005, *Int. J. Remote Sens.*, *29*(22), 6667–6685, doi:10.1080/01431160802168434.

Burt, M. L., G. Wadge, and W. A. Scott (1994), Simple Stochastic modeling of the eruption history of a basaltic volcano: Nyamuragira, Zaire, *Bull. Volcanol.*, *56*(2), 87–97.

Carn, S. A., and G. J. S. Bluth (2003), Prodigious sulfur dioxide emissions from Nyamuragira volcano, D.R. Congo, *Geophys. Res. Lett.*, *30*(23), 2211, doi:10.1029/2003GL018465.

Chakrabarti, R., A. R. Basu, A. P. Santo, D. Tedesco, O. Vaselli (2009a), Isotopic and geochemical evidence for a heterogeneous mantle plume origin of the Virunga volcanics, Western rift, East African Rift system, *Chem. Geol.*, *259*, 273–289, doi:10.1016/j.chemgeo.2008.11.010.

Chakrabarti, R., K. W. W. Sims, A. R. Basu, M. Reagan, and J. Durieux (2009b), Timescales of magmatic processes and eruption ages of the Nyiragongo volcanic from ^{238}U-^{230}Th-^{226}Ra-^{210}Pb disequilibria, *Earth Planet. Sci. Lett.*, *288*, 149–157, doi:10.1016/j.epsl.2009.09.017.

Chorowicz, J., J. Le Fournier, and G. Vidal (1987), A model for rift development in Eastern Africa, *Geol. J.*, *22*(S2), 495–513, doi:10.1002/gj.3350220630.

Coombs, M. L., T. W. Sisson, and P. W. Lipman (2006), Growth history of Kilauea inferred from volatile concentrations in submarine-collected basalts, *J. Volcanol. Geotherm. Res.*, *151*, 19–49, doi:10.1016/j.jvolgeores.2005.07.037.

Couch, S., R. S. J. Sparks, and M. R. Carroll (2003), The kinetics of degassing-induced crystallization at Soufriere Hills Volcano Montserrat, *J. Petrol.*, *44*(8), 1477–1502.

Danyushevsky, L. V., F. N. Della-Pasqua, and S. Sokolov (2000), Re-equilibration of melt inclusions trapped by magnesian olivine phenocrysts from subduction-related magmas: petrological implications, *Contrib. Mineral. Petrol.*, *138*, 68–83.

Danyushevsky, L., A. W. McNeill, and A. V. Sobolev (2002), Experimental and petrological studies of melt inclusions in phenocrysts from mantle-derived magmas: An overview of techniques, advantages, and complications, *Chem. Geol.*, *183*, 5–24, doi:10.1016/S0009-2541(01)00369-2.

Denaeyer, M. E. (1969), Nouvelles donnees lithologiques sur les volcans actifs des Virunga (Afrique Centrale), *Bull. Volcanol.*, *33*(4), 1128–1144, doi:10.1007/BF02597712.

Devine, J. D., H. Sigurdsson, A. N. Davis, and S. Self (1984), Estimates of sulfur and chlorine yield to the atmosphere from volcanic eruptions and potential climatic effects, *J. Geophys. Res.*, *89*(B7), 6309–6325, doi:10.1029/JB089iB07p06309.

Dixon, J. E. (1997), Degassing of alkalic basalts, *Am. Mineral.*, *82*, 368–378.

Dixon, J. E., and V. Pan (1995), Determination of the molar absorptivity of dissolved carbonate in basanitic glass, *Am. Mineral.*, *80*, 1339–1342.

Dixon, J. E., E. M. Stolper, and J. R. Holloway (1995), An experimental study of water and carbon dioxide solubilities in mid-ocean ridge basaltic liquids. Part I: Calibration and solubility models, *J. Petrol.*, *36*(6), 1607–1631.

Dunbar, N. W., R. L. Hervig, and P. R. Kyle (1989), Determination of pre-eruptive H_2O, F, and Cl contents of silicic magmas using melt inclusions: Examples from Taupo volcanic center, New Zealand, *Bull. Volcanol.*, *51*, 177–184.

Ebinger, C. (1989), Tectonic development of the western branch of the East African Rift system, *Geol. Soc. Am. Bull.*, *101*, 885–903, doi:10.1130/0016-7606(1989)101<0885:TDOTWB>2.3.CO;2.

Ebinger, C., and T. Furman (2002), Geodynamical Setting of the Virunga Volcanic Province, East Africa, *Acta Vulcanol.*, *14*(1–2), 1–8.

Edmonds, M., and T. M. Gerlach (2007), Vapor segregation and loss in basaltic melts, *Geology*, *35*, 751–754.

Furman, T. (1995), Melting of metasomatized subcontinental lithosphere: Undersaturated mafic lava from Rungwe, Tanzania, *Contrib. Mineral. Petrol.*, *122*(1–2), 97–115, doi:10.1007/s004100050115.

Furman, T. (2007), Geochemistry of the East African Rift basalts: An overview, *J. Afr. Earth Sci.*, *48*, 147–160, doi:10.1016/j.jafrearsci.2006.06.009.

Furman, T., and D. Graham (1999), Erosion of lithospheric mantle beneath the East African Rift system: Geochemical evidence from the Kivu volcanic province, *Lithos*, *48*, 237–262, doi:10.1016/S0024-4937(99)00031-6.

Furman, T., J. G. Bryce, J. Karson, and A. Iotti (2004), East African Rift System (EARS) plume structure: Insights from Quaternary mafic lavas of Turkana, Kenya, *J. Petrol.*, *45*(5), 1069–1088, doi:10.1093/petrology/egh004.

Gaetani, G. A., and E. B. Watson (2000), Open system behavior of olivine-hosted melt inclusions, *Earth Planet. Sci. Lett.*, *183*(1–2), 27–41, doi:10.1016/S0012-821X(00)00260-0.

George, R. M., and N. W. Rogers (2002), Plume dynamics beneath the African plate inferred from the geochemistry of the Tertiary basalts of southern Ethiopia, *Contrib. Mineral. Petrol.*, *144*, 286–304, doi:10.1007/s00410-002-0396-z.

George, R. M., N. W. Rogers, and S. Kelley (1998), Earliest magmatism in Ethiopia: Evidence for two mantle plumes in one flood basalt province, *Geology*, *26*(10), 923–926, doi:10.1130/0091-7613(1998)026<0923:EMIEEF>2.3.CO;2.

Gerlach, T. M., and E. J. Graeber (1985), Volatile budget of Kilauea volcano, *Nature*, *313*, 273–277, doi:10.1038/313273a0.

Gerlach, T. M., H. R. Westrich, and R. B. Symonds (1996), Preeruption vapor in magma of the climactic Mount Pinatubo eruption: Source of the giant stratospheric sulfur dioxide cloud, in *Fire and Mud: Eruptions and Lahars of Mount Pinatubo, Philippines*, edited by C. G. Newhall and R. S. Punongbayan, pp. 415–433, Univ. of Wash. Press, Seattle, Wash.

Greenland, P., W. I. Rose, and J. B. Stokes (1985), An estimate of gas emissions and magmatic gas content from Kilauea volcano, *Geochim. Cosmochim. Acta*, *49*(1), 125–129, doi:10.1016/0016-7037(85)90196-6.

Gurenko, A. A., M. Chaussidon, and H. U. Schmincke (2001), Magma ascent and contamination beneath one intraplate volcano: Evidence from S and O isotopes in glass includions and their host clinopyroxenes from Miocene basaltic hyaloclastites southwest of Gran Canaria (Canary Islands), *Geochim. Cosmochim. Acta*, *65*(23), 4359–4374, doi:10.1016/S0016-7037(01)00737-2.

Halmer, M. M., H. U. Schmincke, and H. F. Graf (2002), The annual volcanic gas input into the atmosphere, in particular into the stratosphere: A global data set for the past 100 years, *J. Volcanol. Geotherm. Res.*, *115*, 511–528, doi:10.1016/S0377-0273(01)00318-3.

Hamaguchi, H. (1983), Seismological evidence for magma intrusion during the 1981–1982 Nyamuragira eruption, in *Volcanoes Nyiragongo and Nyamuragira: Geophysical Aspects*, edited by H. Hamaguchi, pp. 35–42, Tohoku Univ., Sendai, Japan.

Hamaguchi, H., and N. Zana (1983), Introduction to volcanoes Nyiragongo and Nyamuragira, in *Volcanoes Nyiragongo and Nyamuragira: Geophysical Aspects*, edited by H. Hamaguchi, pp. 1–6, Tohoku Univ., Sendai, Japan.

Harms, E., and H. U. Schmincke (2000), Volatile composition of the phonolitic Laacher See magma (12,900 yr BP): Implications for syn-eruptive degassing of S, F, Cl, and H_2O, *Contrib. Min. Petrol.*, *138*, 84–98.

Hauri, E. (2002), SIMS analysis of volatiles in silicate glasses, 2: Isotopes and abundances in Hawaiian melt inclusions, *Chem. Geol.*, *183*, 115–141, doi:10.1016/S0009-2541(01)00374-6.

Hayashi, S., M. Kasahara, K. Tanaka, H. Hamaguchi, and N. Zana (1992), Major element chemistry of recent eruptive products from Nyamuragira volcano, Africa (1976–1989), *Tectonophysics*, *209*, 273–276, doi:10.1016/0040-1951(92)90033-3.

Johnson, E. R., P. J. Wallace, K. V. Cashman, H. D. Granados, and A. J. R. Kent (2008), Magmatic volatile contents and degassing-induced crystallization at Volcan Jorullo, Mexico: Implications for melt evolution and the plumbing systems of monogenetic volcanoes, *Earth Planet. Sci. Lett.*, *269*(3–4), 478–487.

Johnson, E. R., P. J. Wallace, K. V Cashman, and H. D. Granados (2010), Degassing of volatiles (H_2O, CO_2, S, Cl) during ascent, crystallization, and eruption at mafic monogenetic volcanoes in central Mexico, *J. Volcanol. Geotherm. Res.*, *197*, 225–238, doi:10.1016/j.jvolgeores.2010.02.017.

Kampunzu, A. B., R. T. Lubala, R. Brousse, J. P. H. Caron, D. Cluzel, L. Lenoble, and P. J. Vellutini (1984), Sur l'eruption du Nyamulagira de decembre 1981 a janvier 1982: Cone et coulee du Rugarambiro (Kivu, Zaire), *Bull. Volcanol.*, *47*(1), 79–105.

Kampunzu, A. B., M. G. Bonhomme, and M. Kanika (1998), Geochronology of volcanic rocks and evolution of the Cenozoic Western Branch of the East African Rift System, *J. Afr. Earth Sci.*, *26*(3), 441–461, doi:10.1016/S0899-5362(98)00025-6.

Kasahara, M. (1983), Near-field tilt measurements related to the 1981–1982 Nyamuragira eruption, in *Volcanoes Nyiragongo and Nyamuragira: Geophysical Aspects*, edited by H. Hamaguchi, pp. 47–54, Tohoku Univ., Sendai, Japan.

Katabarwa, J. B., R. Brousse, R. T. Lubala, and C. Thouin (1986), Construction of Kivandimwe (from February to March 1984), two new adventive cones on the north-west flank of Nyamuragira (Birunga volcanic chain, Zaire), *C. R. Acad. Sci., Ser. II*, *302*, 1249–1252.

Krotkov, N. A., S. A. Carn, A. J. Krueger, P. K. Bhartia, and K. Yang (2006), Band residual difference algorithm for retrieval of SO_2 from the Aura Ozone Monitoring Instrument (OMI), *IEEE Trans. Geosci. Remote Sens.*, *44*(5), 1259–1266, doi:10.1109/TGRS.2005.861932.

Krueger, A. J. (1983), Sighting of El Chichon sulfur dioxide clouds with the Nimbus 7 Total Ozone Mapping Spectrometer, *Science*, *220*(4604), 1377–1379, doi:10.1126/science.220.4604.1377.

le Roux, P. J., S. B. Shirey, E. H. Hauri, M. R. Perfit, and J. F. Bender (2006), The effects of variable source, processes and contaminants on the composition of northern EPR MORB (8–10°N and 12–14°N): Evidence from volatiles (H_2O, CO_2, S) and halogens (F, Cl), *Earth Planet. Sci. Lett.*, *251*, 209–231, doi:10.1016/j.epsl.2006.09.012.

Massare, D., N. Metrich, and R. Clocchiatti (2002), High-temperature experiments on silicate melt inclusions in olivine at 1 atm: Inference on temperatures of homogenization and H_2O concentrations, *Chem. Geol.*, *183*, 87–98, doi:10.1016/S0009-2541(01)00373-4.

Mathez, E. A. (1976), Sulfur solubility and magmatic sulfides in submarine basalt glass, *J. Geophys. Res.*, *81*(23), 4269–4276, doi:10.1029/JB081i023p04269.

Mavrogenes, J. A., and H. S. C. O'Neill (1999), The relative effects of pressure, temperature and oxygen fugacity on the solubility of sulfide of sulfide in magic magmas, *Geochim. Cosmochim. Acta*, *63*(7–8), 1173–1180, doi:10.1016/S0016-7037(98)00289-0.

Metrich, N., and R. Clocchiatti (1996), Sulfur abundance and its speciation in oxidized alkaline melts, *Geochim. Cosmochim. Acta*, *60*(21), 4151–4160, doi:10.1016/S0016-7037(96)00229-3.

Metrich, N., and P. J. Wallace (2008), Volatile abundances in basaltic magmas and their degassing paths tracked by melt inclusions, *Rev. Mineral. Geochem.*, *69*(1), 363–402, doi:10.2138/rmg.2008.69.10.

Metrich, N., P. Allard, N. Spilliaert, D. Andronico, and M. Burton (2004), 2001 flank eruption of the alkali- and volatile-rich primitive basalt responsible for Mount Etna's evolution in the last three decades, *Earth Planet. Sci. Lett.*, *228*, 1–17.

Michael, P. J., and J. G. Schilling (1989), Chlorine in mid-ocean ridge magmas: Evidence for assimilation of seawater-influenced components, *Geochim. Cosmochim. Acta*, *53*, 3131–3143, doi:10.1016/0016-7037(89)90094-X.

Newman, S., and J. B. Lowenstern (2002), *VolatileCalc*: A silicate melt-H_2O-CO_2 solution model written in Visual Basic for Excel, *Comput. Geosci.*, *28*(5), 597–604, doi:10.1016/S0098-3004(01)00081-4.

Parfitt, E. A., and L. Wilson (1994), The 1983–86 Pu'u'O'o' eruption of Kilauea Volcano, Hawaii: A study of dike geometry and eruption mechanisms for a long-lived eruption, *J. Volcanol. Geotherm. Res.*, *59*, 179–205.

Parfitt, E. A., and L. Wilson (1999), A Plinian treatment of fall-out from Hawaiian lava fountains, *J. Volcanol. Geotherm. Res.*, *88*, 67–75, doi:10.1016/S0377-0273(98)00103-6.

Platz, T., S. F. Foley, and L. Andre (2004), Low-pressure fractionation of the Nyiragongo volcanic rocks, Virunga Province, D.R. Congo, *J. Volcanol. Geotherm. Res.*, *136*, 269–295, doi:10.1016/j.jvolgeores.2004.05.020.

Portnyagin, M., R. Almeev, S. Matveev, and F. Holtz (2008), Experimental evidence for rapid water exchange between melt inclusions in olivine and host magma, *Earth Planet. Sci. Lett.*, *272*, 541–552.

Pouclet, A. (1975), Activites du volcan Nyamuragira (Rift ouest de l'Afrique Centrale) evaluation des volumes de materiaux emis, *Bull. Volcanol.*, *39*(3), 466–478, doi:10.1007/BF02597267.

Pouclet, A., and M. Villeneuve (1972), L'eruption du Rugarama (mars-mai 1971) au volcan Nyamuragira (Rep. Zaire), *Bull. Volcanol.*, *36*, 200–221, doi:10.1007/BF02596991.

Roedder, E. (1979), Origin and significance of magmatic inclusions, *Bull. Mineral.*, *102*, 487–510.

Roedder, E. (1984), *Fluid Inclusions*, Mineral. Soc. of Am., Washington, D. C.

Roeder, P. L., and R. F. Emslie (1970), Olivine-liquid equilibrium, *Contrib. Mineral. Petrol.*, *29*(4), 275–289, doi:10.1007/BF00371276.

Rogers, N. W., D. James, S. P. Kelley, and M. De Mulder (1998), The generation of potassic lavas from the Eastern Virunga Province, Rwanda, *J. Petrol.*, *39*(6), 1223–1247, doi:10.1093/petrology/39.6.1223.

Roggensack, K. (2001), Unraveling the 1974 eruption of Fuego volcano (Guatemala) with small crystals and their young melt inclusions, *Geology*, *29*, 911–914, doi:10.1130/0091-7613(2001)029<0911:UTEOFV>2.0.CO;2.

Rowe, M. C., A. J. R. Kent, and R. L. Nielsen (2007), Determination of sulfur speciation and oxidation state of olivine hosted melt inclusions, *Chem. Geol.*, *236*, 303–322, doi:10.1016/j.chemgeo.2006.10.007.

Saal, A. E., E. H. Hauri, C. H. Langmuir, and M. R. Perfit (2002), Vapour undersaturation in primitive mid-ocean-ridge basalt and the volatile content of Earth's upper mantle, *Nature*, *419*, 451–455, doi:10.1038/nature01073.

Sawyer, G. M., S. A. Carn, V. I. Tsanev, C. Oppenheimer, and M. Burton (2008), Investigation into magma degassing at Nyiragongo volcano, Democratic Republic of the Congo, *Geochem. Geophys. Geosyst.*, *9*, Q02017, doi:10.1029/2007GC001829.

Schmincke, H. U., C. Park, and E. Harms (1999), Evolution and environmental impacts of the eruption of Laacher See Volcano (Germany) 12,900 a BP, *Quat. Int.*, *61*, 61–72, doi:10.1016/S1040-6182(99)00017-8.

Self, S., M. R. Rampino, M. S. Newton, and J. A. Wolff (1984), Volcanological study of the great Tambora eruption of 1815, *Geology*, *12*(11), 659–663, doi:10.1130/0091-7613(1984)12<659:VSOTGT>2.0.CO;2.

Sharma, K., S. Blake, and S. Self (2004), SO_2 emissions from basaltic eruptions, and the excess sulfur issue, *Geophys. Res. Lett.*, *31*, L13612, doi:10.1029/2004GL019688.

Shaw, A. M., E. H. Hauri, T. P. Fischer, D. R. Hilton, and K. A. Kelley (2008), Hydrogen isotopes in Mariana arc melt inclusions: Implications for subduction dehydration and the deep-Earth water cycle, *Earth Planet. Sci. Lett.*, *275*, 138–145, doi:10.1016/j.epsl.2008.08.015.

Shaw, A. M., M. D. Behn, S. E. Humphris, R. A. Sohn, and P. M. Gregg (2010), Deep pooling of low degree melts and volatile fluxes at the 85°E segment of the Gakkel Ridge: Evidence from olivine-hosted melt inclusions and glasses, *Earth Planet. Sci. Lett.*, *289*, 311–322, doi:10.1016/j.epsl.2009.11.018.

Shinohara, H. (2008), Excess degassing from volcanoes and its role on eruptive and intrusive activity, *Rev. Geophys.*, *46*, RG4005, doi:10.1029/2007RG000244.

Sisson, T. W., and G. D. Layne (1993), H_2O in basalt and basaltic andesite glass inclusions from four subduction-related volcanoes, *Earth Planet. Sci. Lett.*, *117*(3–4), 619–635, doi:10.1016/0012-821X(93)90107-K.

Smithsonian Institution (1982), Nyamuragira, *Sci. Event Alert Network Bull.*, *7*(1), Washington, D. C.

Smithsonian Institution (2006), Nyamuragira, *Bull. Global Volcanism Network*, *32*(1–3), Washington D. C.

Sobolev, A. V., R. Clocchiatti, and P. Dhamelincourt (1983), Les variations de temperature, de la composition du magma et l'estimation de la pression partielle d'eau pendant la cristallisation de l'olivine dans les oceanites du Piton de la Fournaise (Reunion, eruption de 1966), *C. R. Acad. Sci.*, *296*, 275–280.

Spandler, C., H. St C. O'Neill, and V. S. Kamenetsky (2007), Survival times of anomalous melt inclusions from element diffusion in olivine and chromite, *Nature*, *447*, 303–306, doi:10.1038/nature05759.

Sparks, R. S. J. (1997), Causes and consequences of pressurization in lava dome eruptions, *Earth Planet. Sci. Lett.*, *150*, 177–189, doi:10.1016/S0012-821X(97)00109-X.

Spath, A., A. P. Le Roex, and N. Opiyo-Akech (2001), Plume-lithosphere interaction and the origin of continental rift-related alkaline volcanism—The Chyulu Hills Volcanic Province, Southern Kenya, *J. Petrol.*, *42*(4), 765–787, doi:10.1093/petrology/42.4.765.

Spera, F. J., and S. C. Bergman (1980), Carbon dioxide in igneous petrogenesis: I, *Contrib. Mineral. Petrol.*, *74*, 55–66, doi:10.1007/BF00375489.

Spilliaert, N., P. Allard, N. Metrich, and A. V. Sobolev (2006), Melt inclusion record of the conditions of ascent, degassing, and extrusion of volatile-rich alkali basalt during the powerful 2002 flank eruption of Mount Etna (Italy), *J. Geophys. Res.*, *111*, B04203, doi:10.1029/2005JB003934.

Suh, C. E., J. F. Luhr, and M. S. Njome (2008), Olivine-hosted glass inclusions from Scoriae erupted in 1954–2000 at Mount Cameroon volcano, West Africa, *J. Volcanol. Geotherm. Res.*, *169*, 1–33, doi:10.1016/j.jvolgeores.2007.07.004.

Sutton, A. J., T. Elias, T. M. Gerlach, and J. B. Stokes (2001), Implications for eruptive processes as indicated by sulfur dioxide emissions from Kilauea Volcano, Hawaii, 1979–1997, *J. Volcanol. Geotherm. Res.*, *108*, 283–302.

Swanson, D. A., W. A. Duffield, D. B. Jackson, and D. W. Peterson (1979), Chronological narrative of the 1969–1971 Mauna Ulu eruption of Kilauea volcano, Hawaii, *U.S. Geol. Surv. Prof. Pap.*, *1056*, 1–55.

Tedesco, D., O. Vaselli, P. Papale, S. A. Carn, M. Voltaggio, G. M. Sawyer, J. Durieux, M. Kasereka, and F. Tassi (2007), January 2002 volcano-tectonic eruption of Nyiragongo volcano, Democratic Republic of Congo, *J. Geophys. Res.*, *112*, B09202, doi:10.1029/2006JB004762.

Ueki, S. (1983), Recent volcanism of Nyamuragira and Nyiragongo, in *Volcanoes Nyiragongo and Nyamuragira: Geophysical Aspects*, edited by H. Hamaguchi, pp. 7–18, Tohoku Univ., Sendai, Japan.

Vergniolle, S., and C. Jaupart (1990), Dynamics of degassing at Kilauea Volcano, Hawaii, *J. Geophys. Res.*, *95*(B3), 2793–2809, doi:10.1029/JB095iB03p02793.

Vigouroux, N., P. J. Wallace, and A. J. R. Kent (2008), Volatiles in high-K magmas from the Western Trans-Mexican Volcanic Belt: Evidence for fluid fluxing and extreme enrichment of the mantle wedge by subduction processes, *J. Petrol.*, *49*(9), 1589–1618, doi:10.1093/petrology/egn039.

Wallace, P. J. (2001), Volcanic SO_2 emissions and the abundance and distribution of exsolved gas in magma bodies, *J. Volcanol. Geotherm. Res.*, *108*, 85–106, doi:10.1016/S0377-0273(00)00279-1.

Wallace, P. J. (2005), Volatiles in subduction zone magmas: Concentrations and fluxes based on melt inclusion and volcanic gas data, *J. Volcanol. Geotherm. Res.*, *140*, 217–240, doi:10.1016/j.jvolgeores.2004.07.023.

Wallace, P., and A. T. Anderson (1998), Effects of eruption and lava drainback on the H_2O contents of basaltic magmas at Kilauea Volcano, *Bull. Volcanol.*, *59*(5), 327–344, doi:10.1007/s004450050195.

Wallace, P., and S. E. Carmichael (1992), Sulfur in basaltic magmas, *Geochim. Cosmochim. Acta*, *56*, 1863–1874, doi:10.1016/0016-7037(92)90316-B.

Wallace, P. J., and T. M. Gerlach (1994), Magmatic vapor source for sulfur dioxide released during volcanic eruptions: Evidence from Mount Pinatubo, *Science*, *265*(5171), 497–499, doi:10.1126/science.265.5171.497.

Wallace, P. J., A. T. Anderson, and A. M. Davis (1999), Gradients in H_2O, CO_2 and exsolved gas in a large-volume silicic magma system: Interpreting the record preserved in melt inclusions from the Bishop Tuff, *J. Geophys. Res.*, *104*, 20,097–20,122, doi:10.1029/1999JB900207.

Waters, C. L., J. G. Bryce, and T. Furman (2004), Magmatic processes beneath the East African Rift System (EARS): Insights from melt inclusions in lavas of Turkana, Kenya, *Eos Trans. AGU*, *85*(17), Jt. Assem. Suppl., Abstract V43B-05.

Wilson, L. (1980), Relationships between pressure, volatile content and eject velocity, *J. Volcanol. Geotherm. Res.*, *8*, 297–313, doi:10.1016/0377-0273(80)90110-9.

Wilson, L., and J. W. Head (1981), Ascent and eruption of basaltic magma on the Earth and Moon, *J. Geophys. Res.*, *86*(B4), 2971–3001, doi:10.1029/JB086iB04p02971.

Witter, J. B., V. C. Kress, and C. G. Newhall (2005), Volcan Popocatepetl, Mexico. Petrology, magma mixing, and immediate sources of volatiles for the 1994-present eruption, *J. Petrol.*, *46*(11), 2337–2366, doi:10.1093/petrology/egi058.

Yang, K., N. A. Krotkov, A. J. Krueger, S. A. Carn, P. K. Bhartia, and P. F. Levelt (2007), Retrieval of large volcanic SO_2 columns from the Aura Ozone Monitoring Instrument: Comparison and limitations, *J. Geophys. Res.*, *112*, D24S43, doi:10.1029/2007JD008825.

Zana, N. (1983), Seismological study of the 1980 Nyamuragira Eruption, in *Volcanoes Nyiragongo and Nyamuragira: Geophysical Aspects*, edited by H. Hamaguchi, pp. 29–33, Tohoku Univ., Sendai, Japan.